(1)

WRDC-TR-89-2122

AD-A212 523

HEAT PIPES FOR SODIUM-SULFER BATTERIES

John R. Hartenstine

Thermacore, Inc.
780 Eden Road
Lancaster, PA 17601

August 1989

Final Report for Period August 1988 - May 1989

AERO PROPULSION AND POWER LABORATORY
WRIGHT RESEARCH AND DEVELOPMENT CENTER
AIR FORCE SYSTEMS COMMAND
WRIGHT-PATTERSON AIR FORCE BASE, OHIO 45433-6563

Unclassified
SECURITY CLASSIFICATION OF THIS PAGE

REPORT DOCUMENTATION PAGE

1a REPORT SECURITY CLASSIFICATION: Unclassified	1b RESTRICTIVE MARKINGS
2a SECURITY CLASSIFICATION AUTHORITY	3 DISTRIBUTION / AVAILABILITY OF REPORT: Approved for Public Release; Distribution is Unlimited.
2b DECLASSIFICATION / DOWNGRADING SCHEDULE	
4 PERFORMING ORGANIZATION REPORT NUMBER(S)	5 MONITORING ORGANIZATION REPORT NUMBER(S): WRDC-TR-89-2122
6a NAME OF PERFORMING ORGANIZATION: Thermacore, Inc. / 6b OFFICE SYMBOL (If applicable): IT434	7a NAME OF MONITORING ORGANIZATION: Aero Propulsion and Power Lab (WRDC/POOS-3) Wright Research and Development Center
6c ADDRESS (City, State, and ZIP Code): 780 Eden Road Lancaster, Pennsylvania 17601	7b ADDRESS (City, State, and ZIP Code): Wright-Patterson AFB, Oh 45433-6563
8a NAME OF FUNDING / SPONSORING ORGANIZATION: DCASR Philadelphia / 8b OFFICE SYMBOL (If applicable): S3910A	9 PROCUREMENT INSTRUMENT IDENTIFICATION NUMBER: F33615-88-C-2892
8c ADDRESS (City, State, and ZIP Code): P.O. Box 7478 Philadelphia, PA 19101-7478	10 SOURCE OF FUNDING NUMBERS: PROGRAM ELEMENT NO. 63221C / PROJECT NO. D822 / TASK NO. 00 / WORK UNIT ACCESSION NO. 32

11 TITLE (Include Security Classification): Heat Pipes for Sodium-Sulfur Batteries

12 PERSONAL AUTHOR(S): Hartenstine, John R.

13a TYPE OF REPORT	13b TIME COVERED	14 DATE OF REPORT (Year, Month, Day)	15 PAGE COUNT
Final	FROM 8/29/88 TO 5/1/89	1989 August	67

16 SUPPLEMENTARY NOTATION: This is a Small Business Innovation Research Program Report, Phase I

17 COSATI CODES			18 SUBJECT TERMS (Continue on reverse if necessary and identify by block number)
FIELD	GROUP	SUB-GROUP	variable conductance heat pipe, titanium, cesium, sodium-sulfur battery, passive

19 ABSTRACT (Continue on reverse if necessary and identify by block number)

The objective of this program was to develop a variable conductance heat pipe (VCHP) for the thermal management of sodium-sulfur batteries. The VCHP maintains the sodium sulfur battery within a specified temperature rise limit (20°C) while the battery discharges a thermal load from 0 watts to 500 watts. A preliminary full scale thermal management design was developed for the sodium-sulfur battery, incorporating the VCHPs and supporting integration hardware. The feasibility of the VCHPs for this application was proved by test.

20 DISTRIBUTION / AVAILABILITY OF ABSTRACT	21 ABSTRACT SECURITY CLASSIFICATION	
☒ UNCLASSIFIED/UNLIMITED ☐ SAME AS RPT. ☐ DTIC USERS	Unclassified	
22a NAME OF RESPONSIBLE INDIVIDUAL: Brian Hager	22b TELEPHONE (Include Area Code): (513) 255-2922	22c OFFICE SYMBOL: WRDC/POOS

DD FORM 1473, 84 MAR — 83 APR edition may be used until exhausted. All other editions are obsolete

SECURITY CLASSIFICATION OF THIS PAGE
Unclassified

The VCHP developed in Phase I utilized titanium as the heat pipe envelope material, and cesium as the heat pipe working fluid. The wick structure was axial grooves. Analysis and test indicate that the VCHP can provide the passive thermal control necessary for the sodium-sulfur battery.

Test data show that with the heat input from Q = 0 watts to Q = 500 watts, the VCHP evaporator temperature increased from 350°C to 385°C. The temperature control range was higher than predicted due to working fluid vapor diffusion into the noncondensible gas and thermal axial conduction into the VCHP reservoir.

Analysis has shown that by utilizing VCHPs for passive temperature control, the sodium-sulfur battery cells will have a lower axial delta-T during discharge than a current louver design. The VCHP thermal management package has the potential to be used in geosynchronous earth orbits (GEO) and low earth orbits (LEO).

PREFACE

The technical monitor for the Phase I SBIR was Mr. Brian Hager (WPAFB). Mr. Hager was responsible for outlining the technical program for sodium-sulfur batteries, and supplied Thermacore with battery requirements, applications and input as to chief development areas.

This work presented herein represents the efforts of the Development Division of Thermacore, Inc. Messrs Peter M. Dussinger and Robert M. Shaubach provided technical and managerial direction on the program. Direct project engineering was supplied by Messrs John R. Hartenstine and James E. Bogart, who worked with Mr. David L. Muth in performance of the actual program hardware fabrication and testing.

TABLE OF CONTENTS

LIST OF FIGURES

LIST OF TABLES

1.0 INTRODUCTION

Sodium-sulfur batteries are used to provide electrical power to satellite systems when the satellite is in solar eclipse. Solar receivers recharge the sodium-sulfur batteries and supply the electrical power to the remaining system in solstice operation.

In a single orbit, the sodium-sulfur battery operation will experience both an endothermic and an exothermic reaction. The endothermic reaction occurs during recharging in the sunlight mode of operation. In an eclipse, the discharge mode of operation, an exothermic reaction takes place causing an increase in battery temperature. Accumulation of this waste heat can cause damage to the battery cells and electrical components on board the satellite.

One industry approach to the thermal management of the sodium-sulfur battery is to incorporate a mechanical louver onto the bottom of the battery casing. This louver can be operated using a stepper motor. The louver is closed during recharge operation and opened to deep space during discharge operation in order to radiate the generated heat.

Disadvantages of the louver concept include the need for additional power to operate the stepper motor, the need for mechanical linkages that could become stuck, and a large battery cell axial delta-T that is imposed when the louver is opened to deep space. When the battery cell operates with a delta-T, the hotter region of the ceramic electrolyte within the battery draws more current due to the decrease in electrical resistivity. A current gradient then exists within the cell. The area of highest current concentration could cause the ceramic electrolyte to degrade faster with respect to the remaining cell. The large battery cell axial delta-T could accelerate the cell degradation and decrease battery cell life if used in a low earth orbit (LEO) application. The LEO application will have an increase in discharge-recharge cycles during a 24-hour period compared to GEO which has one cycle per 24 hours. Eventually this could cause the electrolyte to fail.

Thermal management of the sodium-sulfur battery using gas-controlled variable conductance heat pipes (VCHP) and battery cell heat pipes (BCHP) can provide passive, lightweight efficient temperature control to isothermalize the battery cells.

In this application, the individual VCHP heat load varies from Q = 0 watts (recharge) to Q = 125 watts (discharge) while operating within a 20°C set-point temperature of the nominal operating temperature, 350°C. Four VCHPs are required for the sodium-sulfur battery. Each VCHP will carry 125 watts, therefore the four VCHPs will transfer a total of 500 watts.

During recharge, the VCHP noncondensible gas occupies the condenser and reservoir regions of the heat pipe. The gas in the condenser blankets the heat transfer area making it "inactive". The reservoir is sized to minimize additional vapor pressure required to compress the noncondensible gas out of the condenser and into the reservoir.

When the 125 watt load is input to the individual VCHP evaporator during discharge, the evaporator temperature and vapor pressure will increase. The increased vapor pressure compresses the gas into the reservoir and exposes the "active" heat transfer area of the condenser. This minimizes the evaporator temperature rise.

Battery cell heat pipes were identified as essential components to enhance the heat transfer from the battery cells to the VCHP. Preliminary analysis shows that BCHPs reduce the battery cell axial delta-T. This will increase the battery cell operating life by reducing the current gradient imposed by the axial delta-T.

The results of this program demonstrate the capability of VCHPs to provide passive, lightweight thermal management for sodium-sulfur batteries.

2.0 CONCLUSIONS AND RECOMMENDATIONS

The purpose of the Phase I program was to demonstrate the feasibility of a variable conductance heat pipe for controlling the cell temperature of sodium-sulfur batteries. The program was successful in all respects. A prototype titanium/cesium VCHP was fabricated and tested, proving the VCHP concept.

The specific conclusions during the program are listed below.

- The titanium/cesium VCHP evaporator achieved a set-point temperature control range of 35°C as the heat load from the battery increased from Q = 0 watts to Q = 500 watts.

- Axial thermal conduction in the heat pipe wall and vapor diffusion into the control gas are dominant factors in the operation of the VCHP. These factors increase the set-point temperature control range from 20°C (calculated) to 35°C (measured). The heat leak measured during VCHP recharge was 21 watts. The heat leak measured was 16 watts over the 5 watt calculated value. Thermal conduction and vapor diffusion are the cause of the increase.

- The VCHP/battery cell heat pipe thermal management package weighs 5.72 lbs. A weight penalty of 0.59 lbs above the 5.13 lb goal was due to the addition of BCHPs.

- VCHPs combined with battery cell heat pipes (BCHP) can aid in reducing the sodium-sulfur battery cell axial delta-T. Reducing the battery cell axial delta-T will reduce the current gradient imposed on the battery cells. The cyclic life of the battery will therefore be increased. The VCHP/BCHP thermal management scheme will lend itself to low earth orbits (LEO) and geosynchronous earth orbits (GEO).

Additional work is required to develop the VCHP and BCHP for the sodium-sulfur battery application. As a minimum, Thermacore recommends the following work be conducted in Phase II.

- Update the requirements for thermal management of sodium-sulfur batteries.
- Design the VCHP to be hardened to illumination by hostile laser weapons when in LEO.
- Utilize test data to refine the analytical model to accurately calculate the reservoir to condenser volume ratio which will result in a 20°C temperature control range or lower.
- Design the VCHP reservoir geometry such that the diffusion and freezing of vapor into the reservoir is eliminated.
- Increase the noncondensible gas charge in order to decrease the heat leak.
- Develop a computer model to predict VCHP, BCHP and battery cell transient and steady state performance through discharge and recharge cycling and laser illumination.
- Continue to evaluate methods to reduce heat pipe weight.
- Develop methods to increase the mounting maneuverability of the VCHP onto the battery.
- Fabricate and test a prototype VCHP.

3.0 TECHNICAL APPROACH

The technical approach for this Phase I work effort was divided into four tasks. A description of these tasks is provided below.

- **Task 1.0 - Identification of the Requirements**

The VCHP design requirements were established in a meeting between WPAFB (B. Hager), and Thermacore (J. Hartenstine and P. Dussinger). The design requirements are presented in Section 3.1.

- **Task 2.0 - Prototype Titanium/Cesium VCHP Design**

Passively controlled VCHPs were evaluated in this task. The design which best meets the design criteria established in Task 1.0 is a VCHP with a wick in the reservoir. For this design, the temperature of the reservoir is equal to the temperature of the sink (deep space). The design details are discussed in Section 3.2.

- **Task 3.0 - Fabrication and Test of the Prototype VCHP**

A VCHP was fabricated and tested. The results are presented in Section 3.3.

- **Task 4.0 - Full Scale VCHP Thermal Management Design**

A thermal management package for sodium-sulfur batteries utilizing VCHPs was established. The details are presented in Section 3.4.

3.1 TASK 1.0 IDENTIFICATION OF THE REQUIREMENTS

The VCHP design requirements for sodium-sulfur batteries were discussed and established in a September 27, 1988 meeting at Thermacore, Inc. Present at the meeting were WPAFB (B. Hager), and Thermacore (J. Hartenstine and P. Dussinger).

The design requirements have been determined through analysis and experimentation by Hughes Aircraft Company under a separate contract to AFWAL. The VCHP design requirements were based on data supplied in a Preliminary Design Review for High Energy Density Rechargeable Batteries dated April 27, 1988, by Hughes Aircraft Company. The details of the design goals are listed in Table 1.

TABLE 1. Titanium/Cesium VCHP Design Requirements

Parameter	Magnitude
Cell Diameter	1.396 inches
Cell Length	9.440 inches
Number Cells Per Battery	64
Battery Dimensions	20" x 22" x 12"
Discharge Time	1.2 hours
Recharge Time	22.8 hours
Heat Dissipation Per Cell	7.17 watts
Total Power Rejected During Discharge	500 watts
Heat Leak	32 watts
Operational Temperature Range	320-390°, 350 nominal
Weight	*<5.13 lbs
Maneuverability Within the Spacecraft	Maximize
**Survivability	Hardened to Laser Illumination

*Requirement imposed at the May 17, 1989, Critical Design Review for the HEDRB

**Requirement recently imposed

3.2 TASK 2.0 - PROTOTYPE TITANIUM/CESIUM VCHP DESIGN

The VCHP is designed to operate with a 350°C evaporator temperature over a 22.8 hour time period during the recharge mode of operation. During this time, the battery transfers a power of 0 watts. This assumes a flat-front model where the affects of thermal axial conduction and vapor diffusion are neglected.

During discharge, the VCHP must be capable of rejecting 500 watts with a 20°C VCHP evaporator temperature rise (370°C) over a 1.2 hour time period. In this mode of operation, the increase in heat load from 0 watts to 500 watts will increase the evaporator temperature and working fluid vapor pressure. The increased vapor pressure compresses the noncondensible gas and exposes the condenser area which was blanketed during recharge operation. This provides additional area for heat transfer and minimizes the evaporator temperature rise. As the noncondensible gas is compressed, the area exposed now becomes active and transfers the waste heat by radiation to the sink, deep space (0°C). An illumination of the VCHP operational sequence is shown in Figure 1.

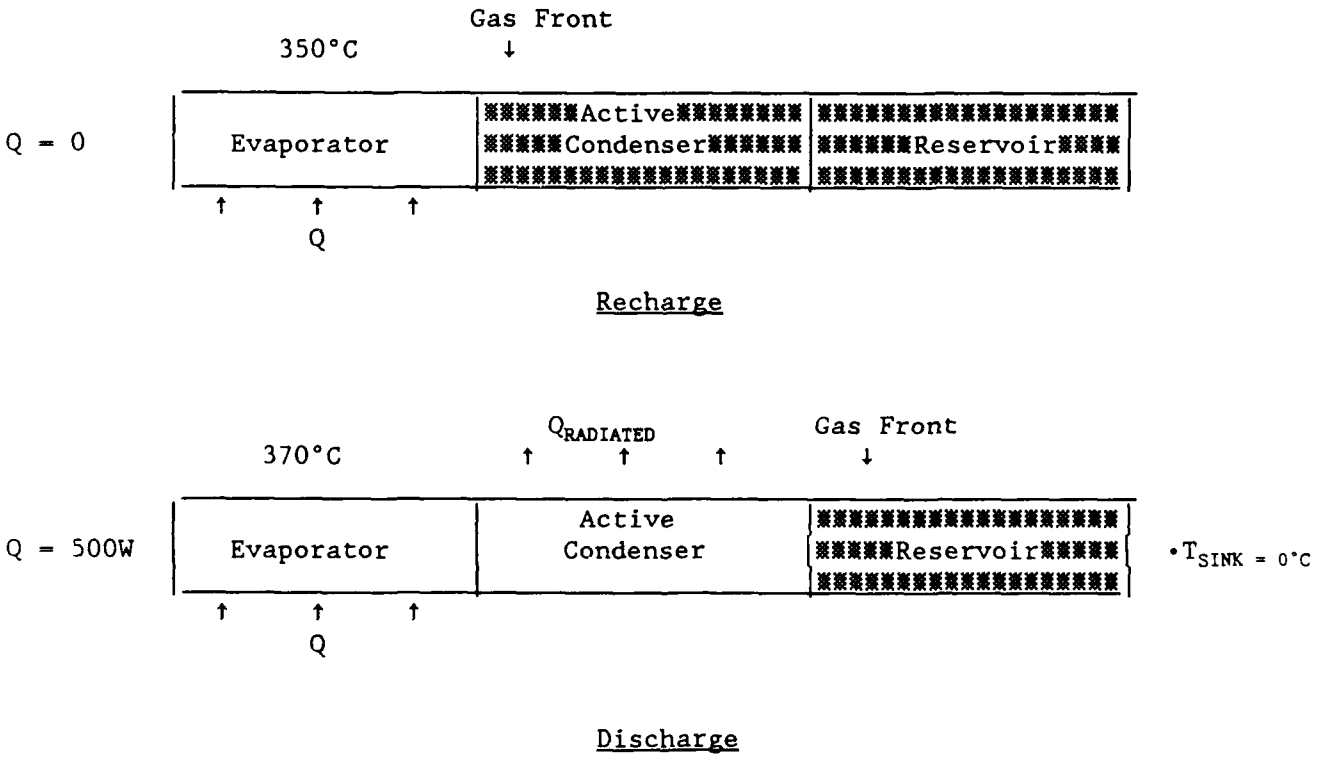

Figure 1. VCHP operational sequence

The VCHP design was divided into the following subtasks:

- VCHP Configuration Evaluation
- Working Fluid Evaluation
- VCHP Design Parameters
- Diffusion of the Working Fluid into the Reservoir

3.2.1 VCHP Configuration Evaluation

Four VCHP configurations were evaluated. The configurations are shown in Figure 2 and include the following:

- VCHP with a wick in the reservoir, $T_{reservoir} = T_{sink}$
- VCHP with a wick in the reservoir, $T_{reservoir} \neq T_{sink}$
- VCHP without a wick in the reservoir, $T_{reservoir} = T_{sink}$
- VCHP with the reservoir coupled to the evaporator, hot reservoir

3.2.1.1 VCHP with a Wick in the Reservoir, $T_R = T_S$

In the VCHP configuration shown in Figure 2a, the gas temperature in the reservoir and condenser are in equilibrium with the sink temperature. A gas reservoir is used to increase the control sensitivity of the gas loaded pipe by minimizing the compression of gas required to move the gas interface. Also, with a reservoir in which a wick is fabricated integral to the reservoir wall, fluid lost to the reservoir from the condenser can be returned to the evaporator via capillary pumping pressure of the wick structure.

3.2.1.2 VCHP with a Wick in the Reservoir, $T_R \neq T_S$

In applications where the sink temperature varies, both the gas temperature in the reservoir changes and the partial pressure of the working fluid vapor in the active portion of the condenser changes. Configurations of this type, Figure 2b, hold the reservoir at a constant temperature to decrease the variations in the heat pipe temperature with fluxuating sink temperatures. Since this configuration is for varying sink conditions, it was not evaluated further.

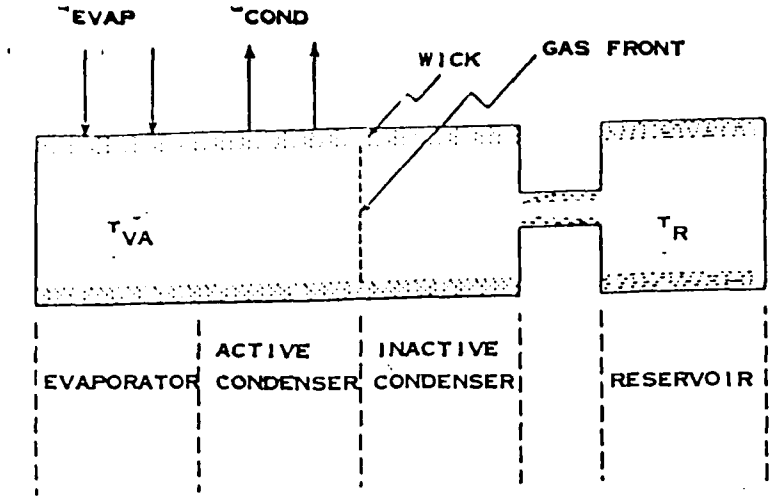

A. VCHP WITH A WICK IN THE RESERVOIR, $T_R = T_S$

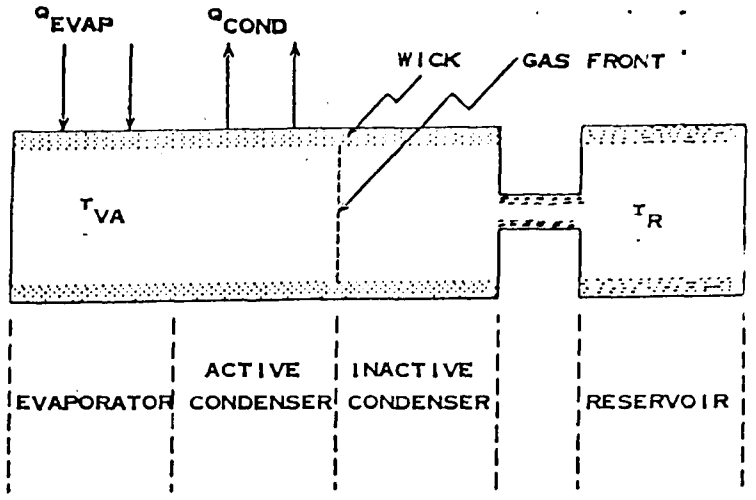

B. VCHP WITH A WICK IN THE RESERVOIR, $T_R \neq T_S$

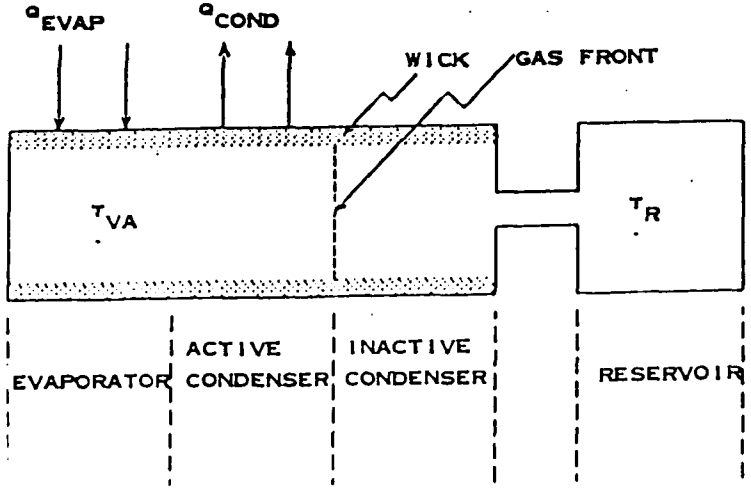

C. VCHP WITHOUT A WICK IN THE RESERVOIR

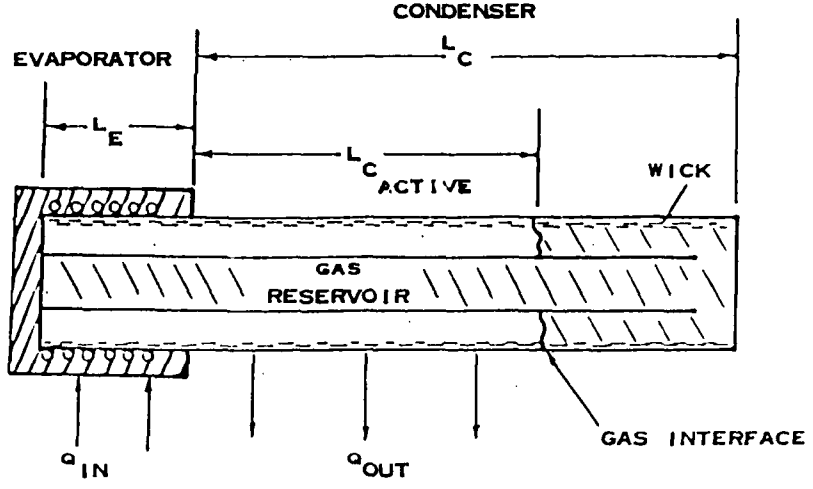

D. VCHP WITH THE RESERVOIR COUPLED TO THE EVAPORATOR HOT RESERVOIR

Figure 2. Alternative VCHP configurations

3.2.1.3 VCHP Without a Wick in the Reservoir

Configurations without a wick in the reservoir shown in Figure 2c, are designed to improve the control of the reservoir temperature independently of varying sink conditions. A drawback of this design is the diffusion of working fluid into the reservoir. Without a wick, working fluid that enters the reservoir by mass diffusion through the noncondensible gas cannot return to the evaporator. Because of this constraint, the VCHP design without a wick in the reservoir was not evaluated further.

3.2.1.4 VCHP With the Reservoir Coupled to the Evaporator, Hot Reservoir

The VCHP configuration with the reservoir coupled to the evaporator is shown in Figure 2d. This type of VCHP provides increased control sensitivity since the reservoir temperature is independent of its surroundings.

The reservoir does not have a wick. With a wick in the reservoir, the vapor pressure is equal to the saturation vapor pressure at the reservoir temperature. In this case, the vapor pressure of the evaporator and reservoir would be essentially equal and the gas would not remain in the reservoir. With a non-wicked reservoir, the vapor pressure of the reservoir is controlled by the partial pressure of the inactive portion of the condenser.

In order to integrate the VCHP reservoir into the evaporator, the evaporator cross section would have to be increased. This would increase the VCHP weight. Since low weight is a primary goal of this Phase I program, this configuration was not evaluated further.

Evaluations of the four VCHP configurations indicate that the preferred design is the VCHP with a wick in the reservoir with $T_R = T_S$. This configuration best meets the operational characteristics for the thermal management of sodium-sulfur batteries.

3.2.2 Working Fluid Evaluation

An evaluation was conducted to select either potassium or cesium as a working fluid. The goal of the evaluation was to determine the fluid which could transfer the power into the smallest cross sectional area. Therefore, the design would have a good chance for weight optimization.

The method of the evaluation was to establish the axial heat flux (Q/A) and corresponding vapor delta-T curves for potassium and cesium. The sonic limit was also calculated for the fluid candidates. The sonic limit is the axial Q/A that occurs when the working fluid reaches sonic velocity.

Increasing the Q/A during heat pipe start-up will produce a large vapor pressure drop in the evaporator, and a corresponding high vapor delta-T. If, at the evaporator exit, there exists a large vapor pressure drop due to a decrease in temperature between the evaporator and condenser, the vapor will increase to sonic velocity. The vapor flow could become choked. This choked condition will limit the heat transfer capability and produce a large vapor delta-T.

The design parameters to avoid a sonic limit include the selection of a working fluid, vapor core area and wick structure. Designing a heat pipe taking into account these design parameters can aid in heat pipe start-up by reducing the affects of a sonic limitation.

The axial heat flux and corresponding vapor delta-T are plotted in Figure 3, along with the sonic limit for potassium and cesium. In comparison with cesium, potassium requires a larger heat pipe cross-sectional area in order to keep the vapor delta-T to a minimum. This large cross-sectional area and associated heavy wall to avoid buckling results in a heavier heat pipe. The heat leak is also increased due to the increased vapor core size. Heat leak is defined as the amount of heat loss due to the axial thermal conduction in the wall material. For the sodium-sulfur battery application, the heat loss during discharge should be minimized in order to maintain the battery temperature.

Weight and heat leak minimization are priority design goals. Therefore, cesium was chosen over potassium as the VCHP working fluid.

3.2.3 VCHP Design Parameters

The VCHP design calculations assume a flat gas front as described by Marcus.[1] The temperature of the reservoir is in equilibrium with the sink temperature. The design incorporates a wick in the reservoir.

---

[1]Marcus, B.D., "Theory and Design of Variable Conductance Heat Pipes: Control Techniques," Contract No. NAS2-5503, Ames Research Center, National Aeronautics and Space Administration, July 1971.

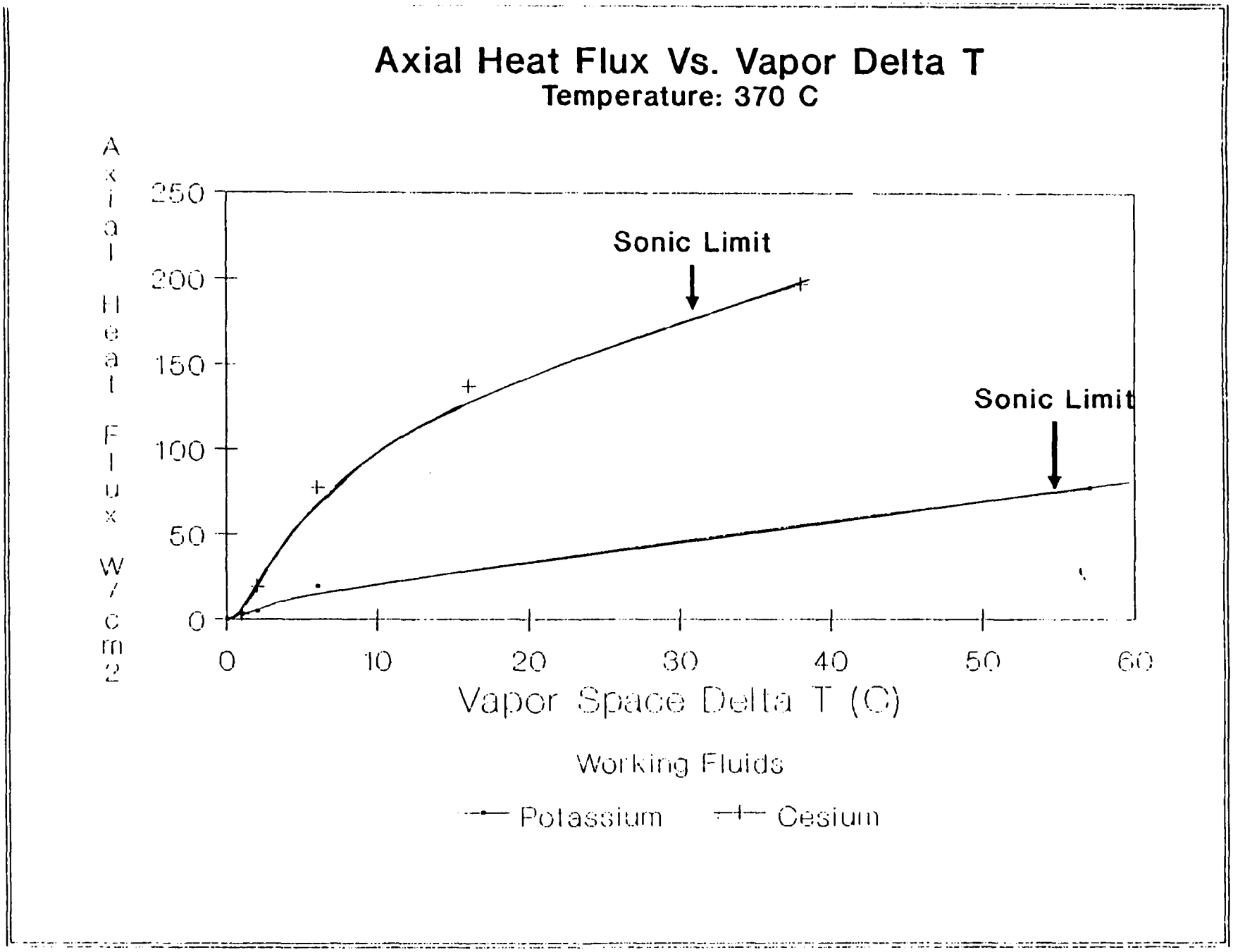

Figure 3. Axial heat flux vs. vapor delta-T

The temperature control range for the VCHP is defined as the difference in evaporator temperatures with the VCHP transporting zero power and then full power. The temperature control range for the VCHP is 20°C.

The temperature control range is dependent upon the reservoir to condenser volume ratio. A plot of the reservoir to condenser volume ratio (V_R/V_C) as a function of temperature control range is shown in Figure 4. A 20°C temperature control range corresponds to a 1.8 V_R/V_C ratio.

The thermal management scheme for the sodium-sulfur battery will utilize four (4) VCHPs. Each VCHP will carry a heat load of 125 watts. The battery will therefore radiate a total of 500 watts.

Argon was selected as the noncondensible gas. Argon is less reactive to alkali metals in comparison with other noncondensible gases such as nitrogen.

As stated in the Phase I proposal, geometric radiating surfaces could be used to increase the surface emissivity and enhance heat rejection due to radiation from the VCHP condenser. Further analysis shows that in order for highly compacted fins or honeycomb panels to raise the surface emissivity, the walls of the cavity should have a high thermal conductivity. A high thermally conductive material is required since the power radiated is a function of the average cavity wall temperature.

The VCHP envelope is titanium. Since titanium has a low thermal conductivity and the addition of geometric radiating surfaces will increase the VCHP weight, geometric radiating surfaces were not utilized.

In order to raise the condenser emissivity, a graphite coating was applied. Data for graphitized carbon indicates an emissivity of 0.70 at 500°C.[2]

The wick structure for the VCHP is rectangular axial grooves. The rectangular grooves were machined longitudinally along the entire VCHP length and were terminated 0.25 inches from each end. This was to prevent the individual grooves from communicating with each other causing the upper grooves to drain when operated in a gravity field.

---

[2]Gubareff, G.G., Janssen, J.E., Turbung, R.H., Thermal Radiation Properties Survey, 2nd Edition, Honeywell Research Center, MA, 1960, Page 55.

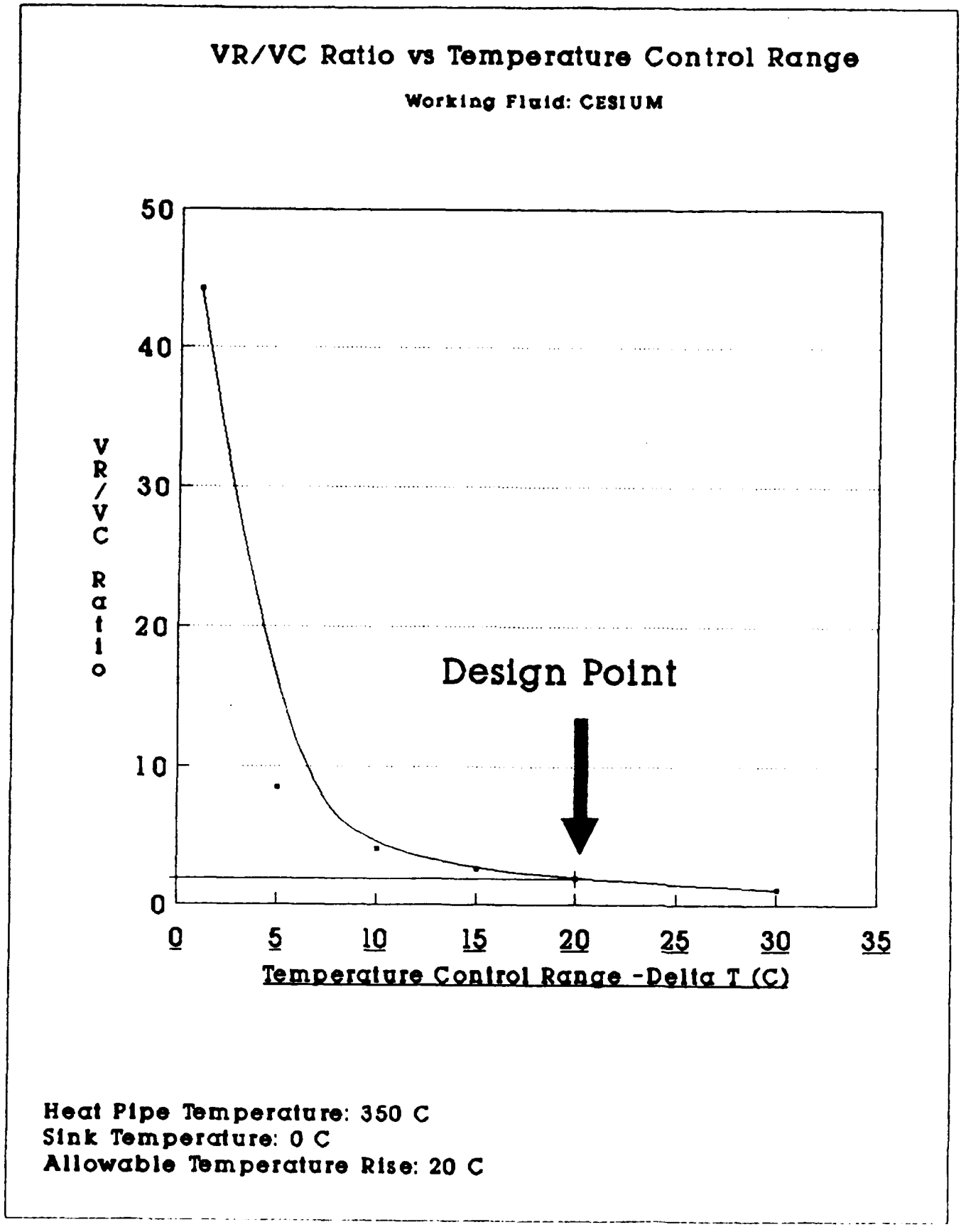

Figure 4. V_R/V_C ratio vs. temperature control range

A computer program entitled "BATTERY" was written by Thermacore to calculate the VCHP design parameters. The program requires an input of 17 variables and calculates the VCHP reservoir and condenser sizes, noncondensible gas charge, heat leak, fin efficiency, mass, and VCHP associated pressure drops and delta-T's.

The design criteria for the VCHP using cesium as the working fluid are listed in Table 2.

TABLE 2. VCHP Design Criteria

Envelope Material	Titanium, CP Grade 2
Working Fluid	Cesium
Evaporator Length	20 inches
Condenser Length	11.067inches
Reservoir Length	20.399 inches
Total Length	51.466 inches
Cross-Section	0.750 inches x 0.750 inches
Noncondensible Gas	Argon
Heat Load (Per Pipe)	125 watts
Operating Temperature	350°C
Acceptable Temperature Rise (Discharge Mode)	20°C
Wick Structure	Axial Grooves
Calculated Weight (Envelope and Fluid)	0.786 lbs
Calculated Heat Leak (Per Pipe)	5 watts
Fin Width (Per Side)	1.750 inches
Fin Length (Per Side)	7.467 inches
Fin Thickness (Per Side)	0.020 inches

3.2.4 Vapor Diffusion Into the Reservoir

An analysis was conducted to determine the diffusion rate of the working fluid into the reservoir at full power (500 watts). Diffusion rate is particularly important since the sink temperature in the reservoir (0°C) is below the freezing point of cesium (28°C). Cesium which is diffused into to the reservoir and freezes will not return to the evaporator via capillary action of the wick. The VCHP will eventually dry out due to lack of fluid.

The estimation of cesium mass transport into the gas reservoir was done using a three-dimensional finite-difference program written at Thermacore. A copy of the computer code and calculation of the diffusion coefficient of cesium into argon is presented in Appendix B. The computer program utilizes a varying mesh size to calculate the temperature profile of the reservoir wall and the cesium concentration profile in the vapor core. For the purpose of the analysis the emissivity of the reservoir was set a 0.6.

The temperature and cesium concentration contours are presented in Figures 5 and 6. The distance from the condenser-reservoir interface at which the reservoir wall temperature reaches the freezing point of cesium (28°C) is 3.8 inches. The mass flux across this plane is 5.652×10^{-8} kg/second. Assuming that the eclipse mode is 72 minutes the calculated freeze-out of cesium is 0.244 grams per eclipse. The working fluid charge for the VCHP is 25 grams. Freezing 0.244 grams of cesium into the reservoir every 24-hour cycle will deplete the VCHP evaporator of working fluid after several cycles.

Four alternate methods are available to thaw the cesium during solstice operation and return the fluid to the evaporator of the VCHP. These methods include solar irradiation, trace heaters, utilizing a working fluid with a melting point lower than 0°C, and geometrically redesigning the VCHP reservoir.

A preliminary one-dimensional finite-difference program was written to determine if solar irradiation could thaw the working fluid over the 22.8 hour solstice time period. The results indicate that the VCHP condenser and reservoir should reach the melting point of cesium during

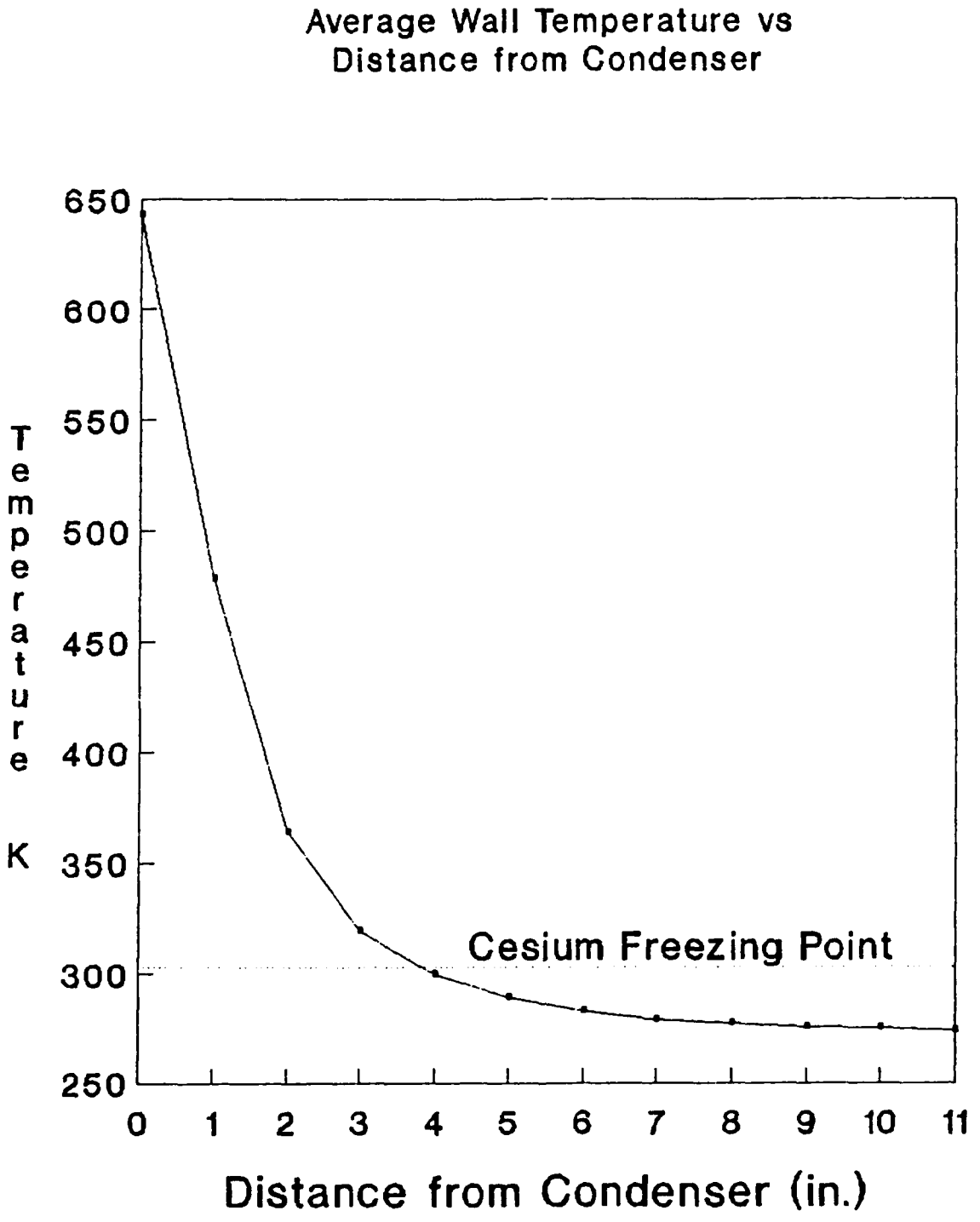

Figure 5. Average wall temperature vs. distance from condenser

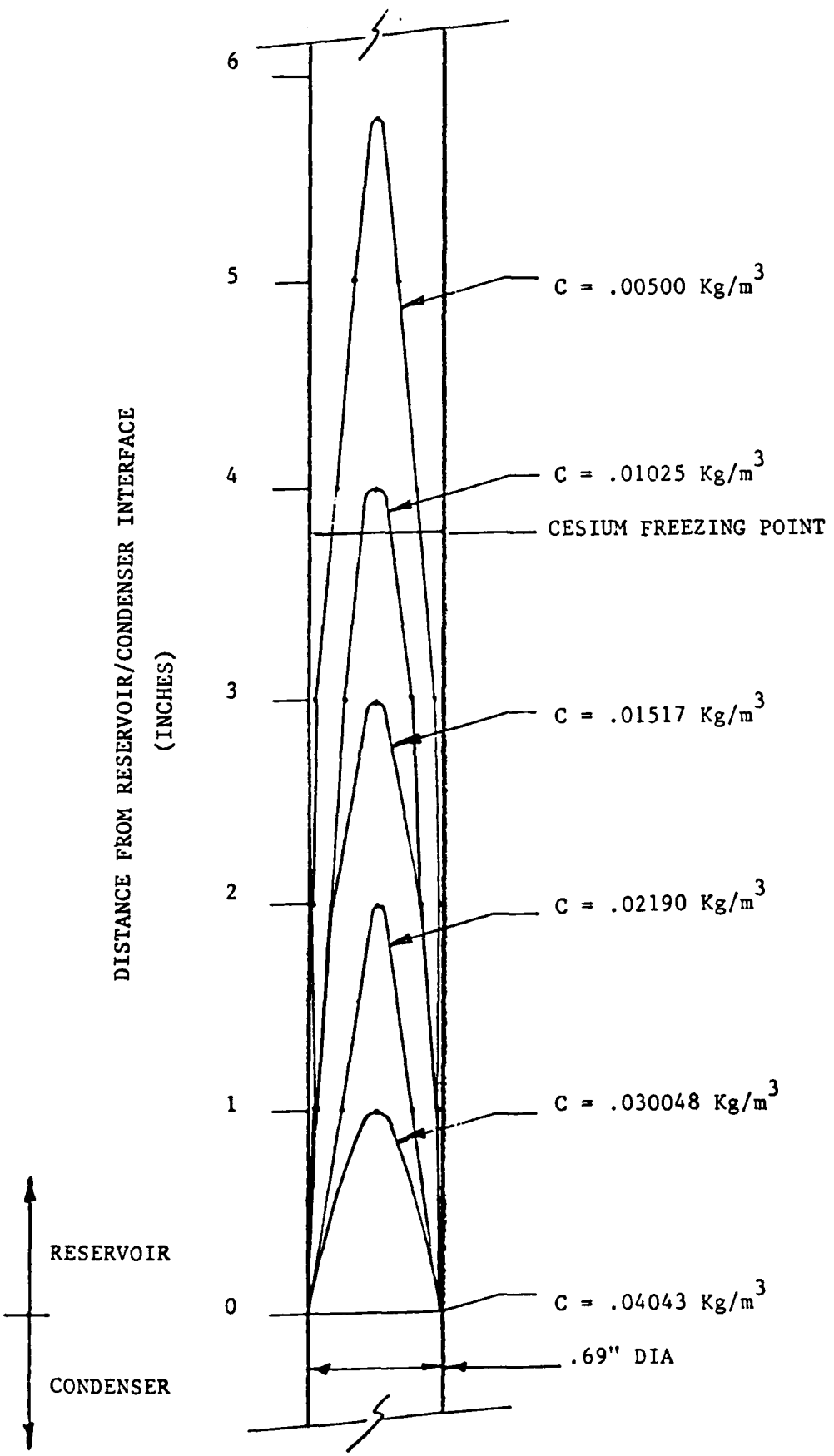

Figure 6. Cesium concentration contours into the reservoir

solstice operation. These results are preliminary. A full scale model is not within the scope of this Phase I work effort. A more detailed analysis is to be conducted in Phase II.

Trace heaters placed over the VCHP reservoir could thaw the frozen cesium. The disadvantage is the need for external power to energize the heaters.

Binary alloys such as cesium-sodium and cesium-potassium have melting points of -30°C and -37.5°C respectively. Using these alloys as working fluids would eliminate the freezing problem in the reservoir. A Phase II work effort would include the thermodynamic analysis of binary and ternary alloys with lower melting points than 0°C.

Redesigning the geometry of the VCHP reservoir will also solve the freezing problem. Shortening the reservoir such that the overall temperature remains above 28°C will keep the cesium from freezing.

These methods of returning the working fluid to the evaporator would also be beneficial if the battery is put into orbit from a warm launch. This could cause the working fluid to move into the reservoir if the temperature reaches 28°C or above. Once positioned in orbit, the fluid could freeze in the reservoir. If the entire working fluid inventory is frozen in the reservoir from launch conditions, the heat pipe would not operate. One of the above methods to thaw the cesium could solve the problem.

3.3 TASK 3.0 - FABRICATION AND TEST OF THE PROTOTYPE VCHP

A prototype titanium/cesium VCHP was fabricated and tested. Individual component and assembly drawings are presented in Appendix A.

Following machining of the wick structure into the VCHP walls, the components were assembled by electron beam welding. A leak check procedure with a helium mass spectrometer verified the weld integrity. A photograph of the VCHP cross-section and overall view is shown in Figures 7-8.

A high temperature bellows valve was assembled onto the fill tube. The valve was used to charge the VCHP with noncondensible gas.

Cesium was loaded into the VCHP. The VCHP was then heated to 400°C in order to remove noncondensible gas present in the working fluid or heat pipe walls.

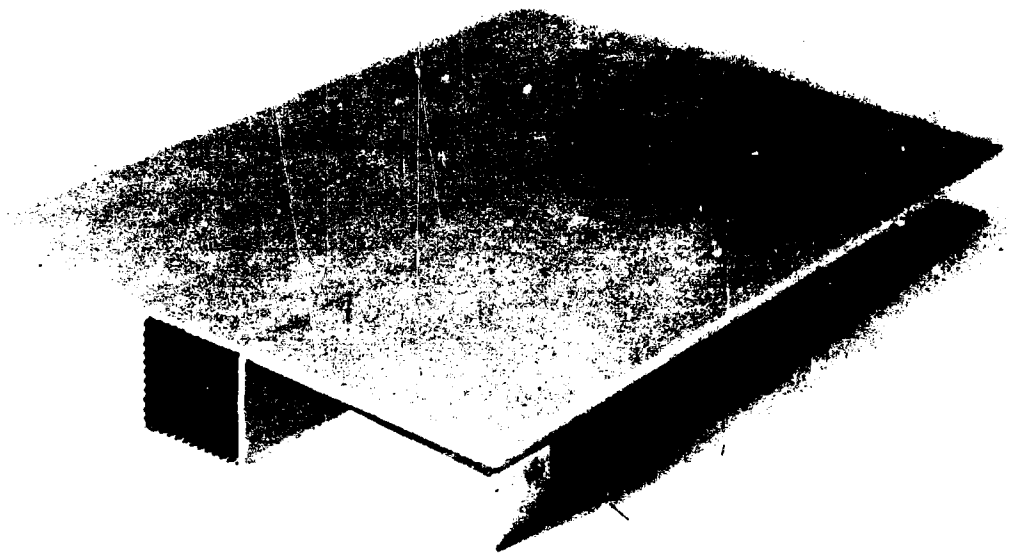

Figure 7. VCHP Cross-section

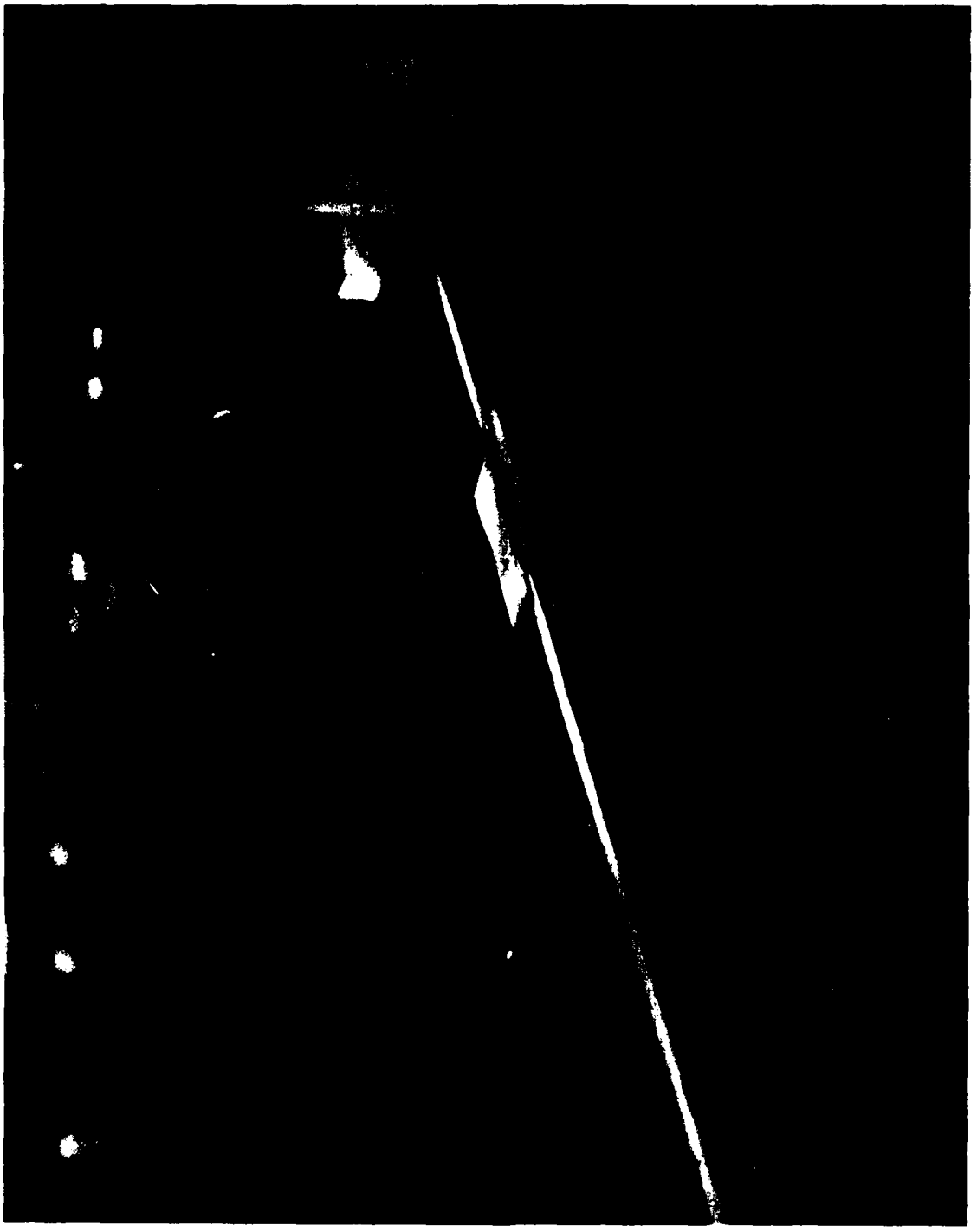

Figure 8. Full length VCHP

3.3.1 Performance Testing Procedure

The VCHP was instrumented with seventeen (17) type "K" thermocouples. Cartridge heaters simulated the thermal load from the sodium-sulfur battery. A copper water cooled jacket was placed around the VCHP condenser and reservoir. The water cooled jacket provided a method for calorimetry measurements, and established a constant sink temperature. The bottom and sides of the condenser were insulated with stainless steel foil in order for the VCHP to radiate from the top only. Figure 9 shows a photograph of the full instrumented VCHP.

The VCHP was tested in a vacuum chamber to simulate a space environment. A vacuum atmosphere of at least 5×10^{-5} torr was attained during performance testing. The test procedure for the VCHP is documented below.

- Apply power to the cartridge heaters evenly until the evaporator reaches 350°C. Record this power value.
- Allow the VCHP to reach a steady state condition and calculate the heat leak using the copper water cooled calorimeter.
- Increase the power 125 watts above the previously recorded power value.
- The Hewlett Packard data acquisition system will record the transient temperature profile of the VCHP during start-up scanning the thermocouples every ten seconds.

3.3.2 Test Results

Test results presented in this section will include test data for VCHP weight, discharge performance and heat leak.

3.3.2.1 VCHP Weight

The total VCHP weight measured 0.740 lbs. The titanium envelope accounted for 0.663 lbs. The cesium mass weighed 0.077 lbs.

3.3.2.2 VCHP Performance During Discharge

The VCHP temperature profile during the 72 minute discharge time period is shown in Figure 10. This graph plots the thermocouple location along the VCHP length versus temperature.

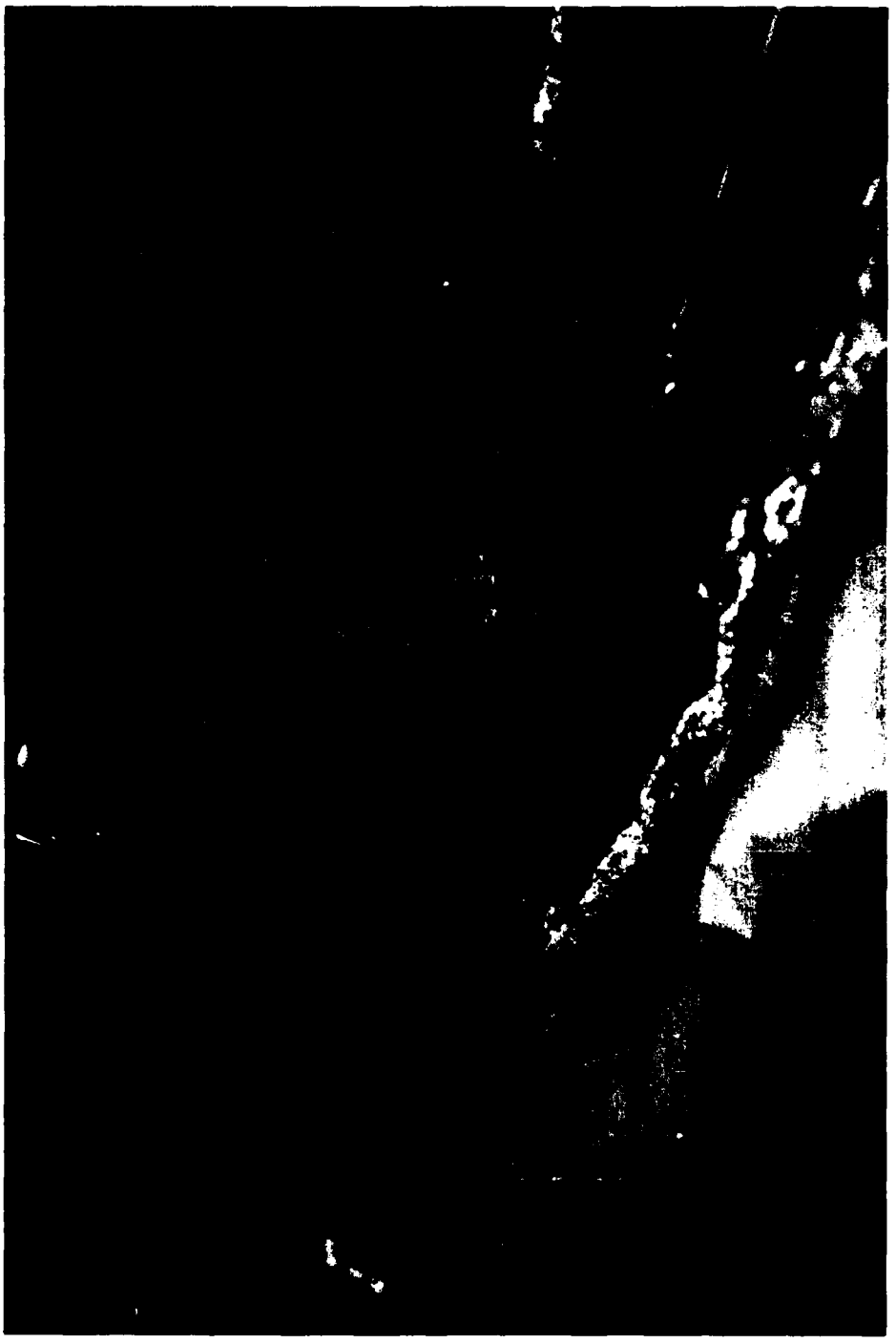

Figure 9. Fully instrumented VCHP

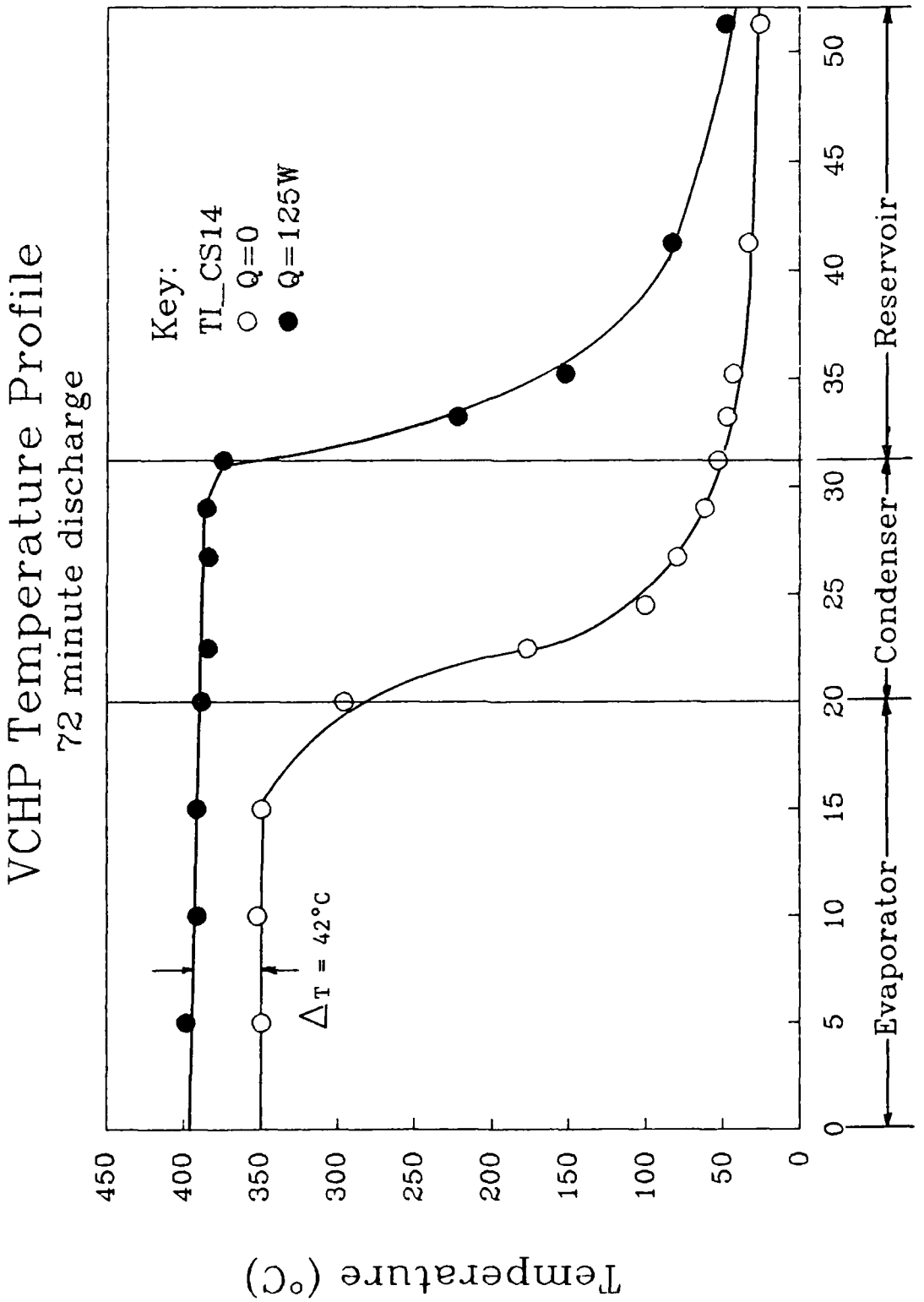

Figure 10. VCHP temperature profile 72-minute discharge test, TI-CS14

The test results show the noncondensible gas interface at both Q = 0 and Q = 125 watt conditions. At Q = 125 watt conditions, the gas interface was pushed into the gas reservoir by the cesium vapor, exposing the radiative portion of the condenser. A temperature control range of 42°C was measured during the 72-minute discharge period. This is 22°C above the design goal of 20°C. The diffusion of vapor into the reservoir and axial conduction are the main cause for the discrepancy.

The diffusion of vapor into the reservoir and axial conduction will increase the active condenser volume and decrease the reservoir volume. This results in a lower reservoir to condenser volume ratio (V_R/V_C) and a higher temperature control range. The V_R/V_C was calculated assuming a flat front model with a sharp interface at the condenser to reservoir transition. The affects of the diffusion and axial conduction limitations are illustrated in Figure 11.

The flat front model assumes an isothermal evaporator and condenser at 370°C. At the condenser to reservoir interface, the temperature of the VCHP decreases to the sink temperature (0°C). The test data from file TI-CS14 is plotted to show the comparison with the flat front model.

The increase in the average reservoir gas temperature and partial pressure of vapor within the gas blocked reservoir cause the VCHP to operate similarly to a hot reservoir VCHP model. The V_R/V_C for a VCHP model in which the reservoir is coupled to the evaporator was calculated for various temperature control ranges. Figure 12 plots V_R/V_C versus temperature control range for both the hot and cold reservoir models. Test data show the VCHP to follow the operational characteristics of a hot reservoir model.

A revised diffusion coefficient was calculated, utilizing the computer program written to calculate the vapor diffusion and temperature profile into the reservoir, and actual test data. The original diffusion coefficient calculated was 19.67 cm^2/sec. This calculation is shown in Appendix B. The diffusion coefficient derived from the test data is 23.2 cm^2/sec.

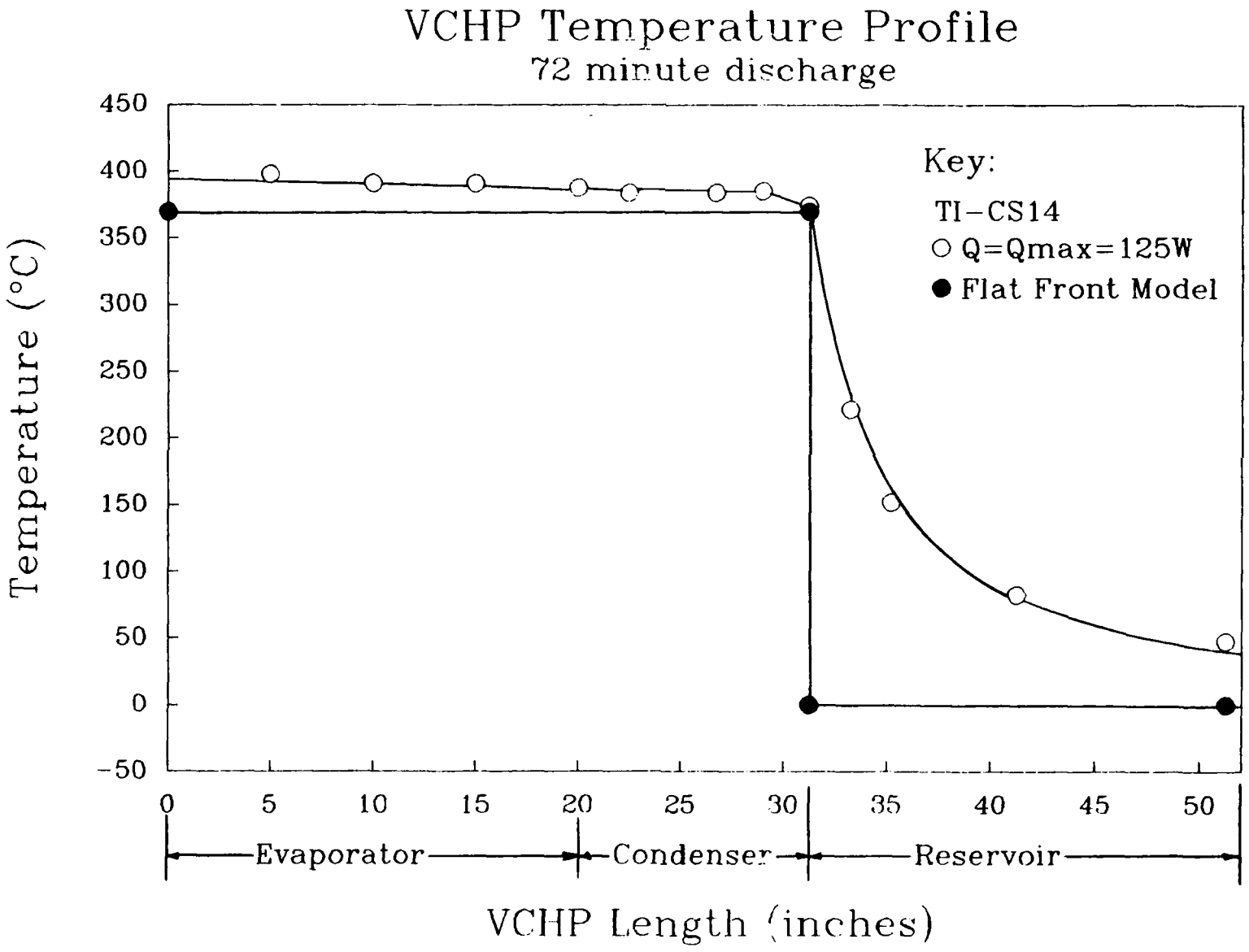

Figure 11. VCHP temperature profile 72-minute discharge flat front model and experimental data

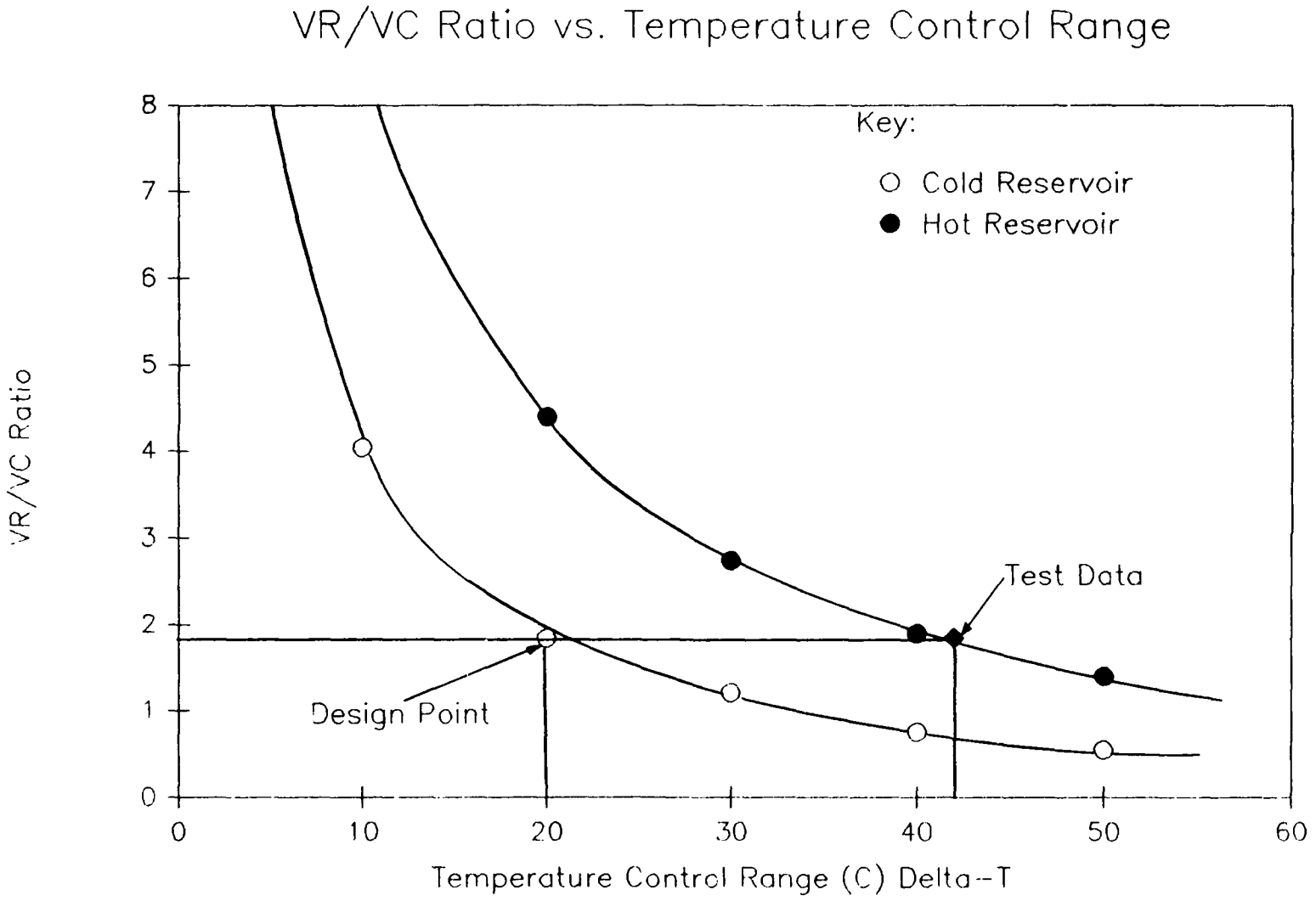

Figure 12. V_R/V_C ratio vs. temperature control range, hot and cold reservoir models

The analysis to determine a revised diffusion coefficient, showed the reservoir emissivity used in the computer model to be higher than that of the actual heat pipe. The model assumed an emissivity of a 0.6. The VCHP is fabricated from titanium. A published value of oxidized titanium is 0.11.[3] To increase the emissivity, the reservoir area was coated with graphitized carbon and the VCHP was re-tested. The increase in the emissivity lowered the temperature control range from 42°C to 35°C. The temperature profile also followed the computer program predictions. A plot showing the VCHP temperature profile versus length for a VCHP reservoir emissivity equal to 0.6 is shown in Figure 13.

The calculation for the VCHP area estimated a fin efficiency of 1.0. The actual fin efficiency was 0.50. The revised fin efficiency was determined by test and analysis. Using the 0.50 fin efficiency, the radiator area was recalculated. The results indicated that the radiating area was approximately 33% less than required to radiate 125 watts.

The insulation surrounding the bottom of the condenser was removed in order to increase the radiating area. The VCHP was re-tested. A comparison was made between the temperature control range with the insulation in place and with the insulation removed. The test data indicated a decrease in the temperature control range of only 1-2°C with the insulation removed.

3.3.2.3 Heat Leak

Heat leak for the VCHP is defined as the heat loss due to axial thermal conduction in the heat pipe wall. For the sodium-sulfur battery application, the heat loss during recharge, sunlight mode of operation should be minimized in order to maintain the battery temperature.

The heat leak calculated for the VCHP was 5 watts. The measured heat leak was 21 watts. The cause for the measured heat leak to be four times higher than predicted is associated with the diffusion of vapor into the gas blocked zone of the condenser. Again, the increase in the reservoir gas temperature extends the radiating surface of the condenser adding to the heat leak.

---

[3]Gubareff, G.G., J.E. Janssen, R.H. Turbung, Thermal Radiation Properties Survey, 2nd edition, Honeywell Research Center, Minneapolis, Minnesota, 1960, page 160.

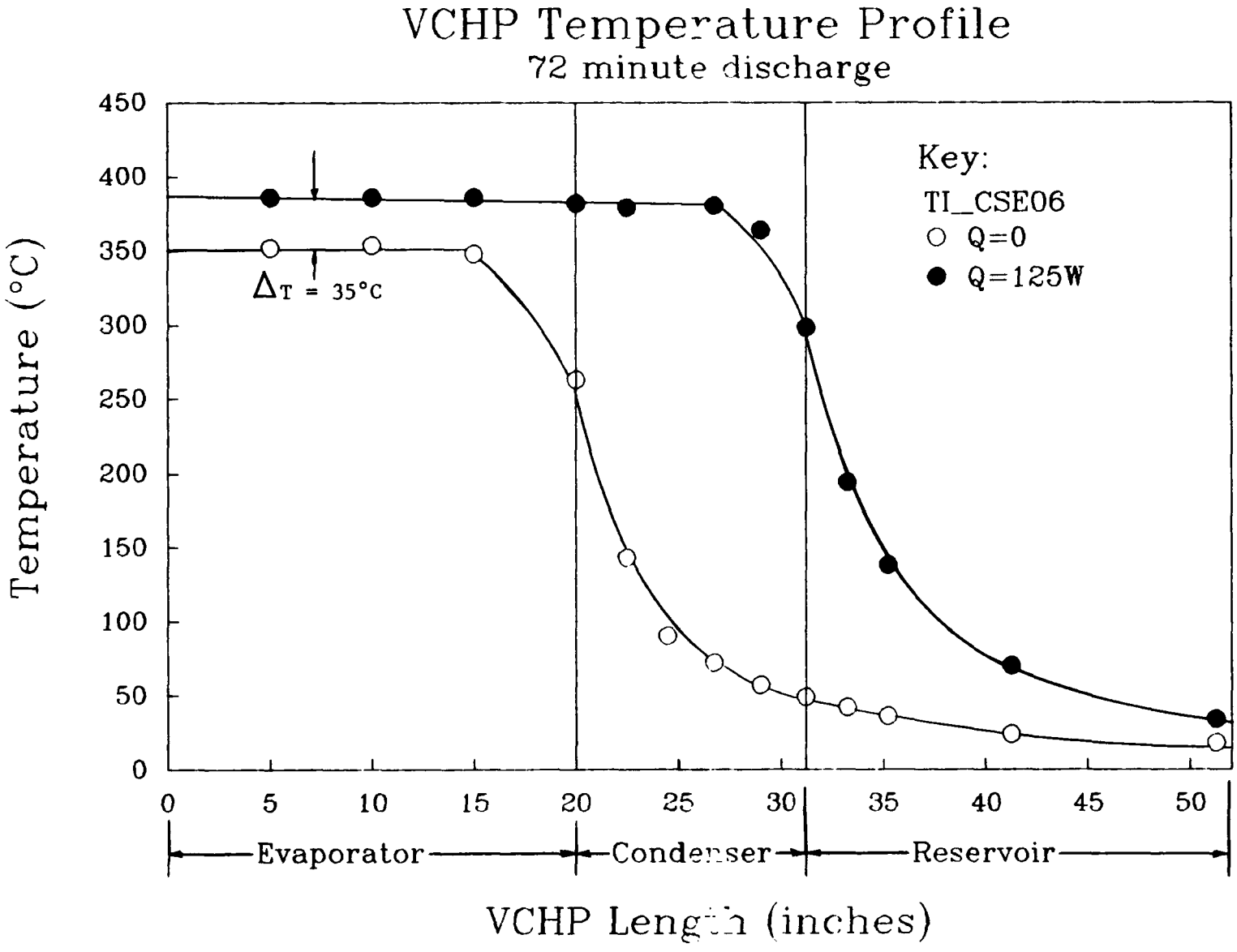

Figure 13. VCHP temperature profile 72-minute discharge reservoir $\epsilon = 0.6$

One method to decrease the high heat leak would be to increase the gas volume in the VCHP. Increasing the gas volume will move the gas interface further into the evaporator during Q = 0 watt conditions. This is shown graphically in Figure 14. In this figure, actual test data are compared to a hypothetical performance curve where the gas volume has been increased. Moving the gas interface further into the evaporator will decrease the heat leak.

3.3.2.4 Recommendations

In order to achieve the required 20°C temperature control range set point, the V_R/V_C ratio should be increased. Since the VCHP operates similarly to a hot reservoir model, the V_R/V_C should be increased from 1.8 to approximately 4.4 as shown in Figure 13.

The increase in V_R/V_C will increase the VCHP weight. The amount of the increase will depend upon the reservoir design geometry.

3.4 TASK 4.0 - FULL-SCALE VCHP THERMAL MANAGEMENT DESIGN

Two VCHP designs have been selected to determine the better method of integration of the VCHPs into the sodium-sulfur battery. The first design integrates only the VCHPs onto the sodium-sulfur battery. This design was evaluated in order to compare the thermal management design using VCHPs to the thermal management design which uses a mechanical louver. The second integration design utilizes both VCHPs and battery cell heat pipes to provide battery thermal management. Isothermalizing the battery cell ceramic electrolyte and weight reduction are the prime design criteria.

3.4.1 Integration: VCHP Only

The VCHPs will be mounted directly to a battery cell support panel located on the bottom of the sodium-sulfur battery (Figure 15). The VCHPs will be fixtured with fins extending from both sides of the evaporator wall (Figure 16). The mounting fins will be incorporated with a series of holes. The hole alignment will match those holes already designed into the battery cell support panel. The hardware used to mount

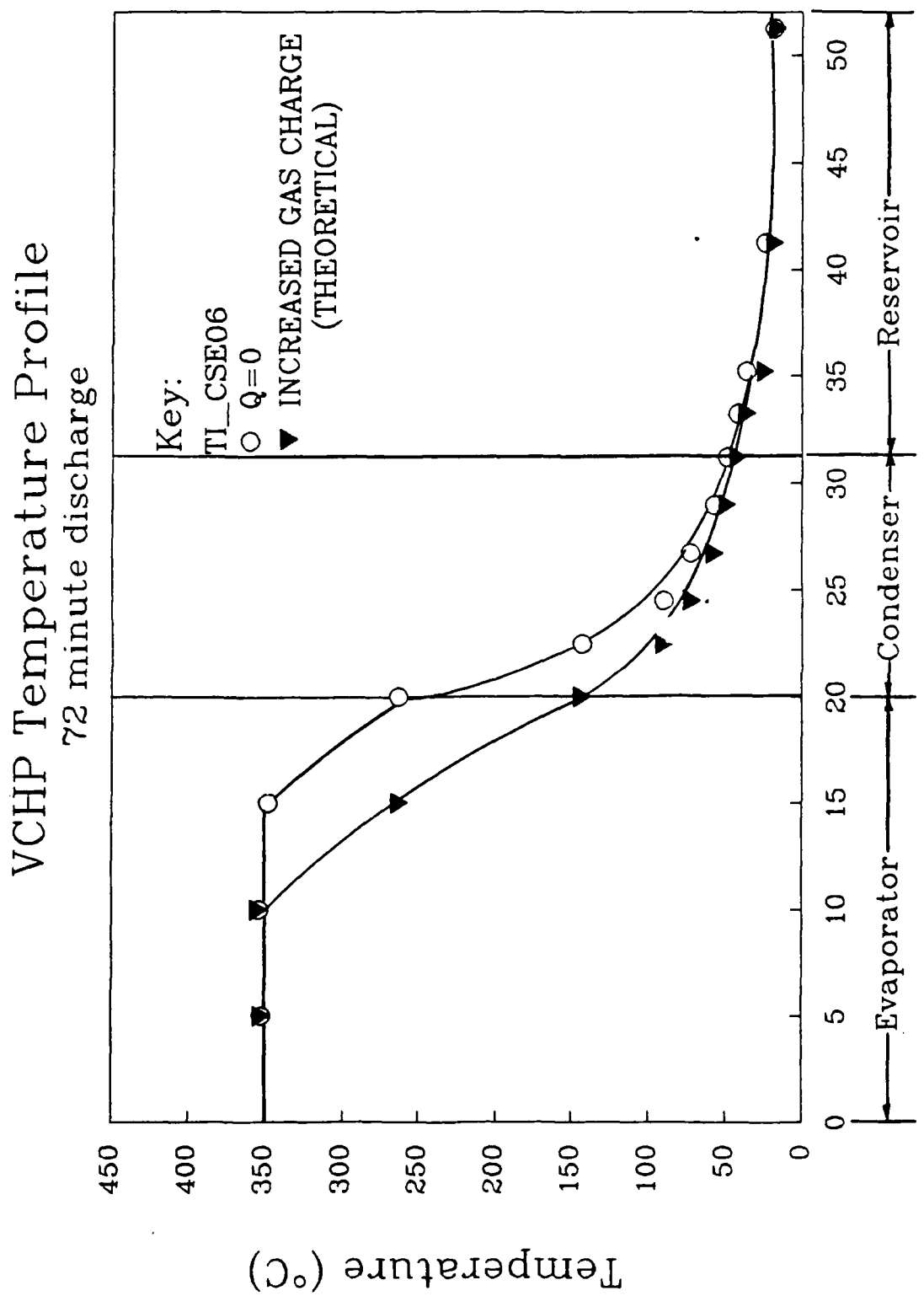

Figure 14. Example of increasing the gas charge to decrease the heat leak

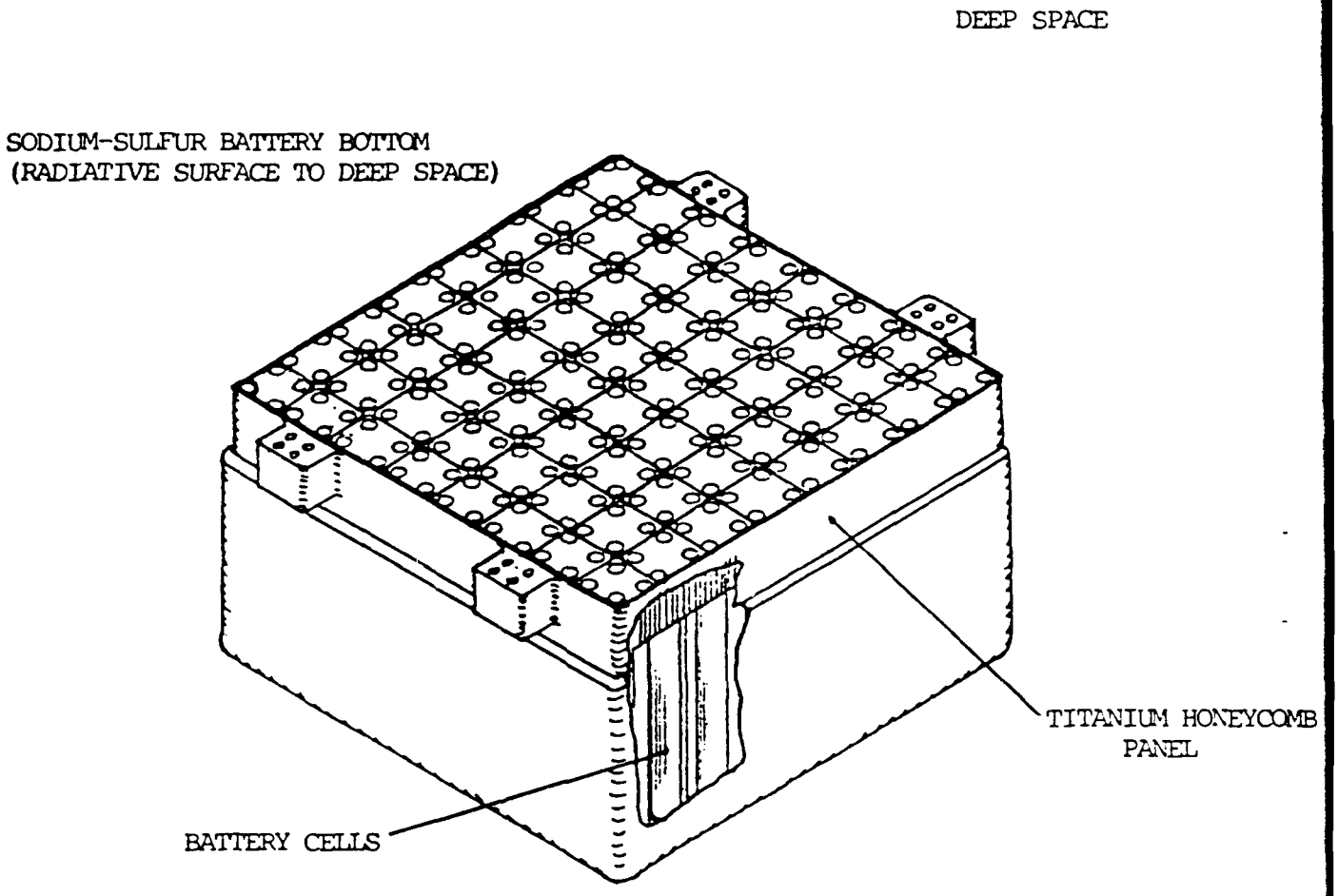

Figure 15. Sodium-sulfur battery

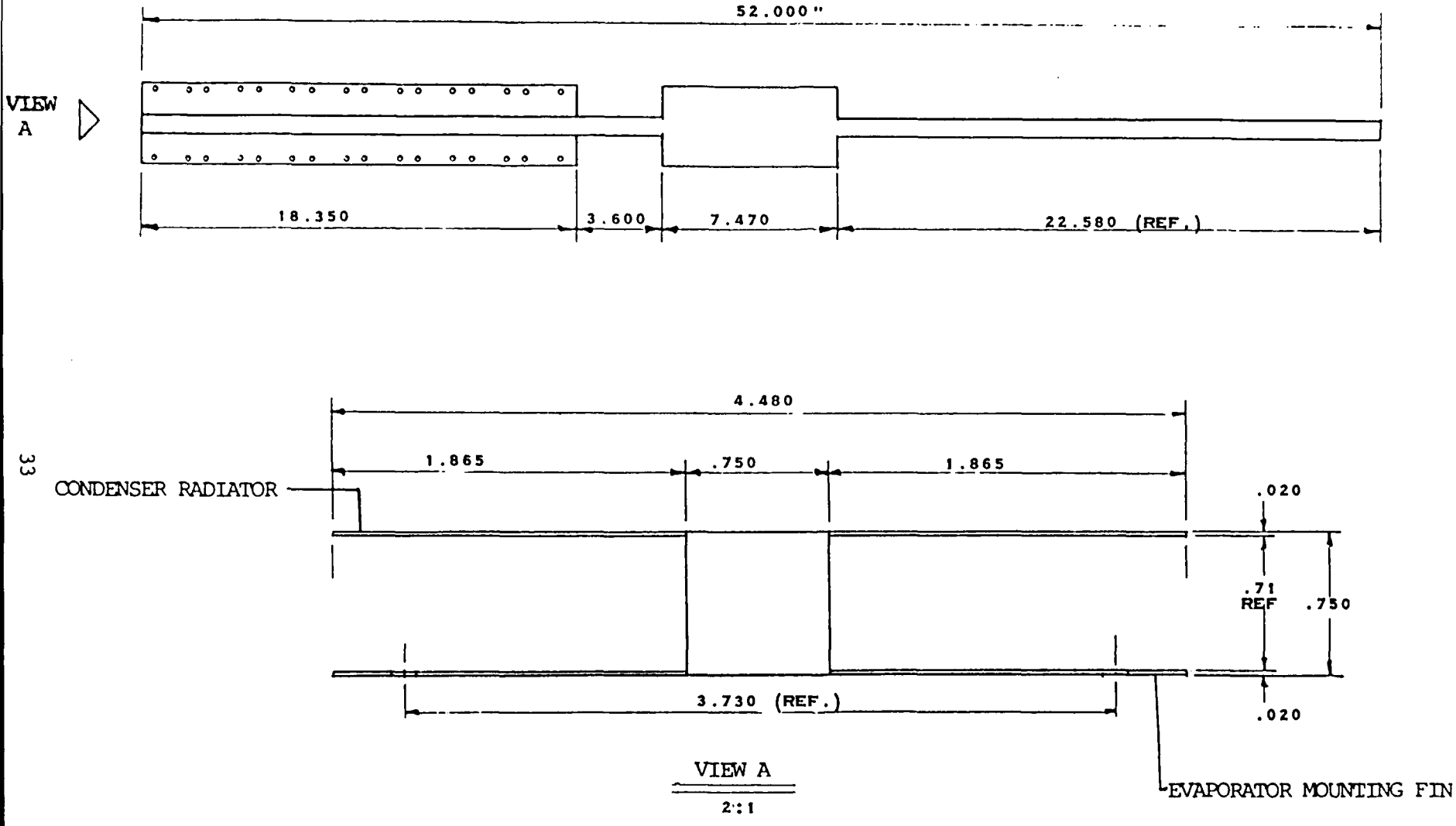

Figure 16. VCHP mounting design

the battery cells will also be used to mount the VCHPs. Figure 17 and 18 show the VCHP mounting arrangement. Layers of insulation will be placed over the VCHPs and mounting fins. The purpose of the insulation is to provide a means of maintaining the battery cell temperature at 325°C during recharge, and provide a uniform evaporator temperature during discharge.

A preliminary thermal analysis was conducted on the two integration designs. The purpose for the analysis was to compare the temperature profile of the battery cells and VCHP with the results of a thermal model using a mechanical louver during the 72 minute discharge time period.

A temperature profile of the mechanical louver concept is shown in Figure 19.[4] This figure indicates the typical battery cell temperature profile versus time during discharge. At 0.5 hours into the discharge cycle, the louver is opened and the waste heat is radiated from the bottom of the battery to deep space. At 1.2 hours, the louver door is closed.

Figure 19 plots three curves. These curves include the battery cell base temperature, battery cell bottom temperature and the battery cell bulk temperature. During discharge, the base cell temperature decreases from 325°C to 283°C. The bottom cell temperature increases from 325°C to 355°C. The bulk cell temperature increases from 325°C to 387°C. The delta-T within the active portion of the battery is 32°C (T_{bulk} - T_{bottom}).

Reducing the battery cell axial delta-T has advantages if the sodium-sulfur battery is used in a low earth orbit (LEO). The LEO application will increase the number of battery cell discharge - recharge cycles compared to a geosynchronous earth orbit (GEO). Reducing the battery axial delta-T could increase the life of the battery as described below.

A sodium-sulfur battery cell operating with an axial delta-T in the ceramic electrolyte will result in the hotter area of the electrolyte to have a lower electrical resistivity. The decrease is the electrical resistivity will increase the current draw in the hot area of the electrolyte. This will result in a current gradient over the battery cell

---

[4]"High Emissivity Density Rechargeable Battery, Critical Design Review," Hughes Aircraft Company, Contract #F33615-86-C-2601, May 17, 1989.

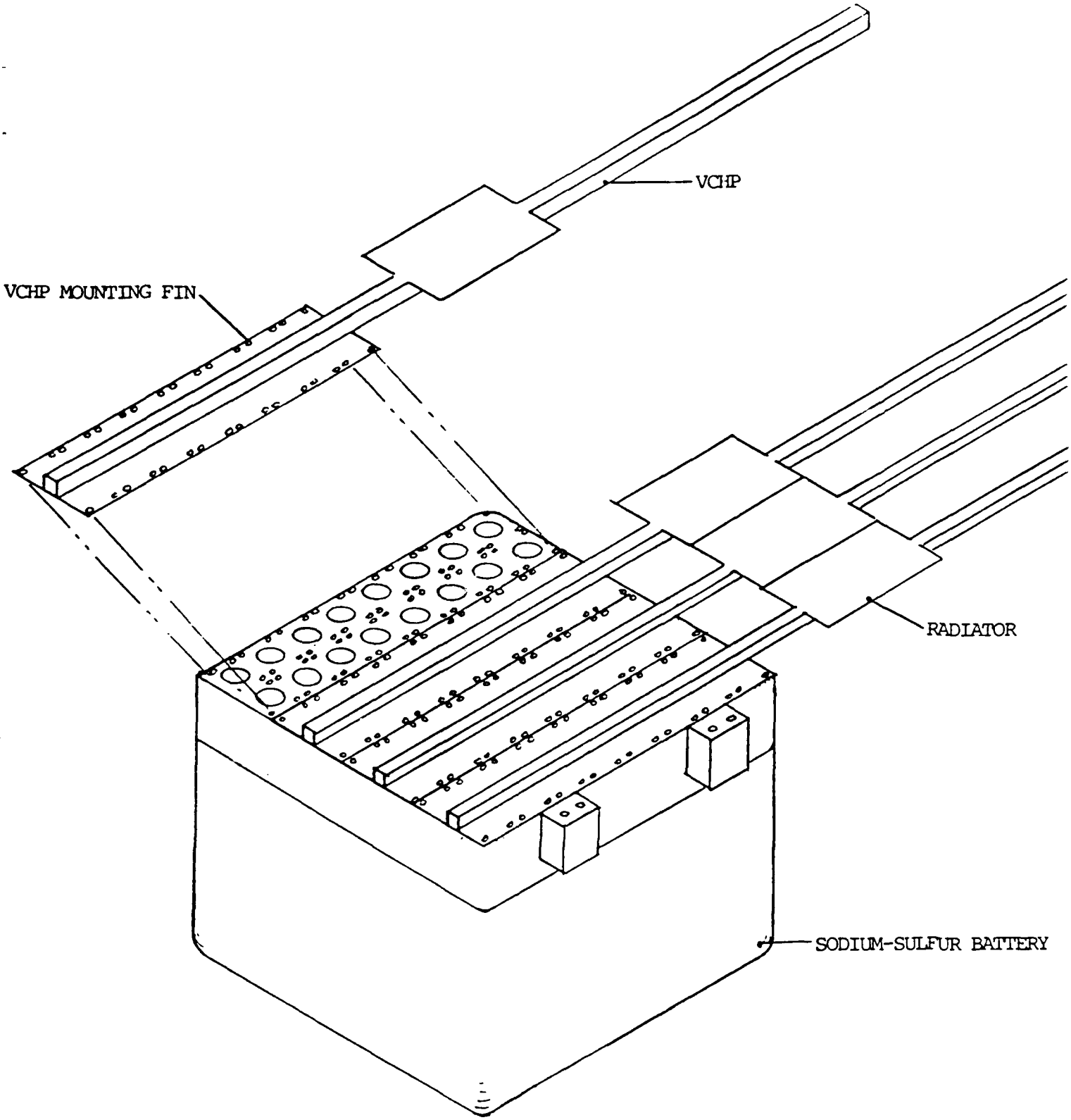

Figure 17. VCHP integration with the sodium-sulfur battery

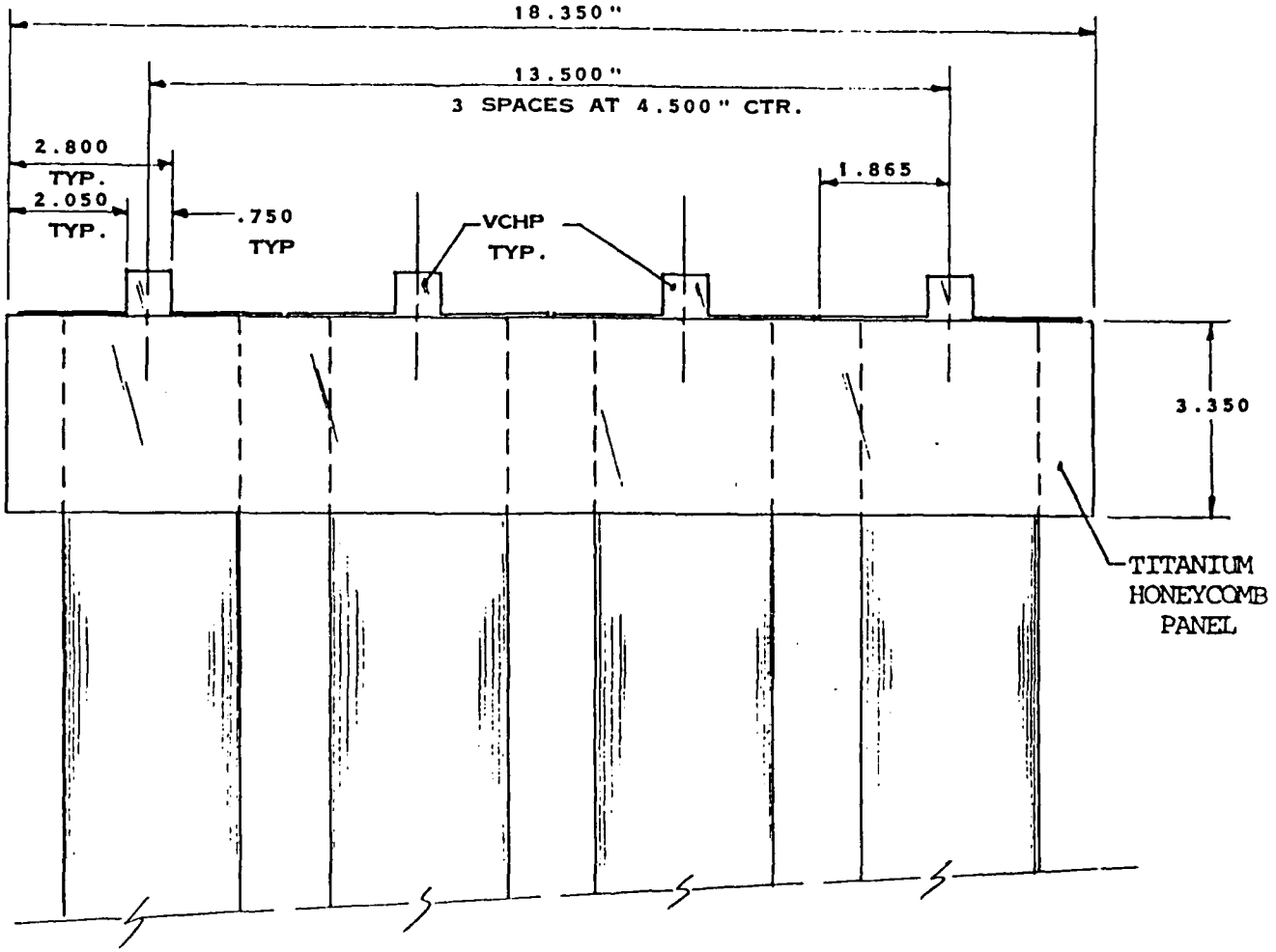

Figure 18. VCHP/Sodium-sulfur battery integration

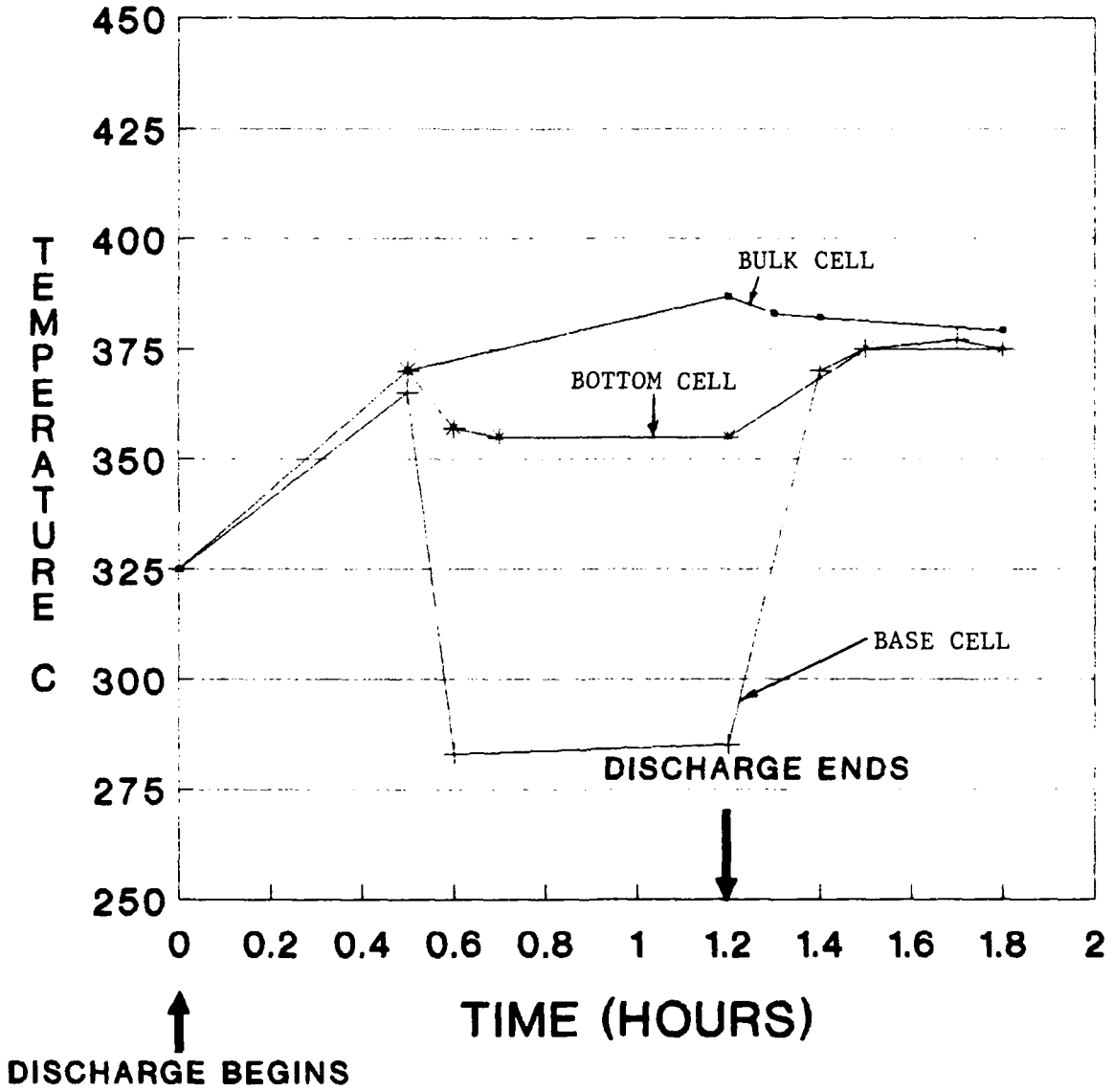

Figure 19. Sodium/sulfur battery temperature profiles - 71 minute discharge cycle - louver design

life of the ceramic electrolyte. The hotter area could degrade faster than the remaining ceramic electrolyte. Therefore, the provision of a thermal management system capable of reducing the battery cell axial delta-T would aid in providing long cyclic life for the sodium-sulfur cells in LEO and GEO applications.

The results of the analysis using VCHPs only is shown in Figure 20. In the preliminary analysis, radiation was assumed to be the mechanism for transferring heat from the cells to the battery cell support panel. A more formal model was not developed due to time and monetary considerations. A complete thermal model will be developed in Phase II.

During discharge the VCHP evaporator and base cell temperatures will increase from 325°C to 345°C. This increase is a result of the 20°C temperature control range designed into the VCHP when the battery cell power changes from Q = 0 watts to Q = 500 watts. The beginning of discharge temperature of 325°C was selected in order to compare the VCHP and louver thermal models. The bulk cell temperature will increase from 325°C to 419°C. The bulk cell temperature using VCHP is higher than that for the louver design because the battery cells are radiating to a 345°C sink temperature while the louver design is radiating to a sink temperature of 283°C.

The bulk cell temperature (419°C) is above the peak cell temperature requirement of 404°C. The integration design concept with VCHPs cannot be used due to the excessive bulk cell temperature. Battery cell heat pipes are therefore required as described below.

3.4.2 Integration: VCHPs and Battery Cell Heat Pipes

Integration of the VCHP and battery cell heat pipe (BCHP) combination into the sodium-sulfur battery is similar to the integration scheme used for VCHPs only. The VCHP will be fixtured with mounting fins on the evaporator. The VCHP will mount directly on the bottom of the battery using the existing holes to mount the battery cells. The mounting design is shown in Figures 15-18.

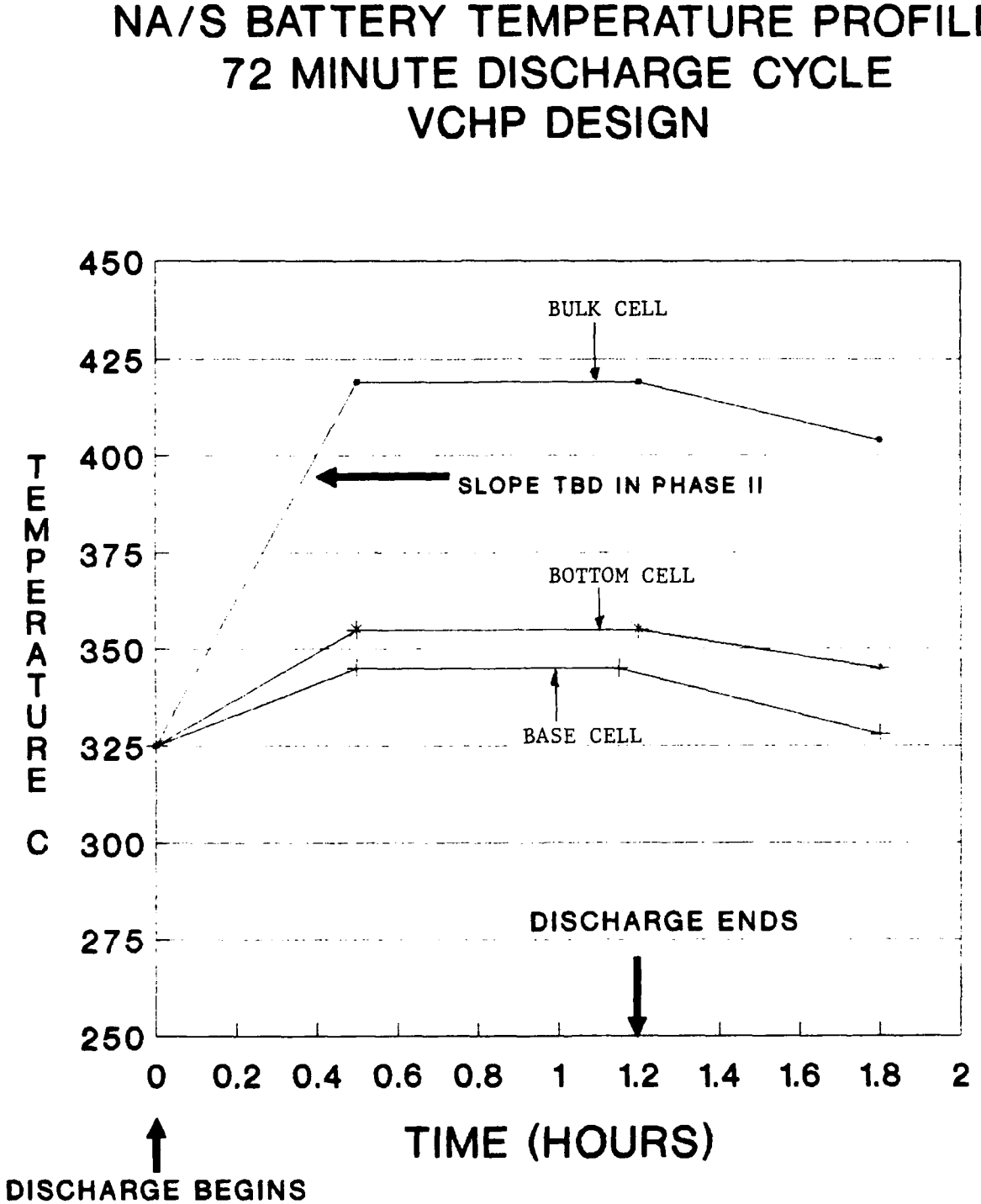

Figure 20. Na/S battery temperature profile - 72 minute discharge cycle - VCHP design

The BCHPs will be inserted through holes machined into the battery cell support panel. They will be positioned equal distant from the battery cells. It was determined through a phone conversation with WPAFB (B. Hager, Technical Monitor) that the battery cell support panel can be altered from its original design to accommodate the BCHPs. The position of the BCHPs within the battery will not conflict with the cells or wiring.

A drawing of the BCHP is shown in Figure 21. The preliminary BCHP design will be fabricated from a 0.375" diameter x .025" wall x 9.440" long titanium envelope. The wick structure will be sintered powder metal bonded to the inside diameter of the heat pipe. The working fluid will be cesium. The BCHP will be fixtured with fins in order to enhance the radiation exchange between the battery cells and the BCHP. Aluminum was used as the preliminary fin material due to its low density and high thermal conductivity. A Phase II work effort would investigate attachment techniques in order to overcome the thermal expansion mismatch between the titanium heat pipe envelope and aluminum fins.

The condenser of the BCHP will be mounted directly into the VCHP evaporator as shown in Figure 22. The VCHP and BCHP are separate heat pipes having separate distinct vapor core areas. The BCHP is mounted directly into the VCHP in order to minimize large interface delta-T's caused by contract resistances. The outside diameter of the BCHP condenser will have a sintered powder metal wick bonded to the heat pipe wall. The purpose of the wick is to maintain the liquid return path from the VCHP condenser to the evaporator via axial grooves. Part of a Phase II program will be a study to determine the affects of the vapor pressure drop in the VCHP evaporator when adding BCHPs. The BCHP evaporator will extend through the support panel and between the battery cells are shown in Figure 23.

A preliminary thermal analysis using VCHPs and BCHPs was conducted. In this analysis, the radiation exchange from battery cells to the battery cell support panel with the addition of battery cell heat pipes will enhance the heat transfer from the battery cells. Figure 24 shows a temperature profile during discharge of the bulk cell temperature, the bottom cell temperature, and the base cell temperature.

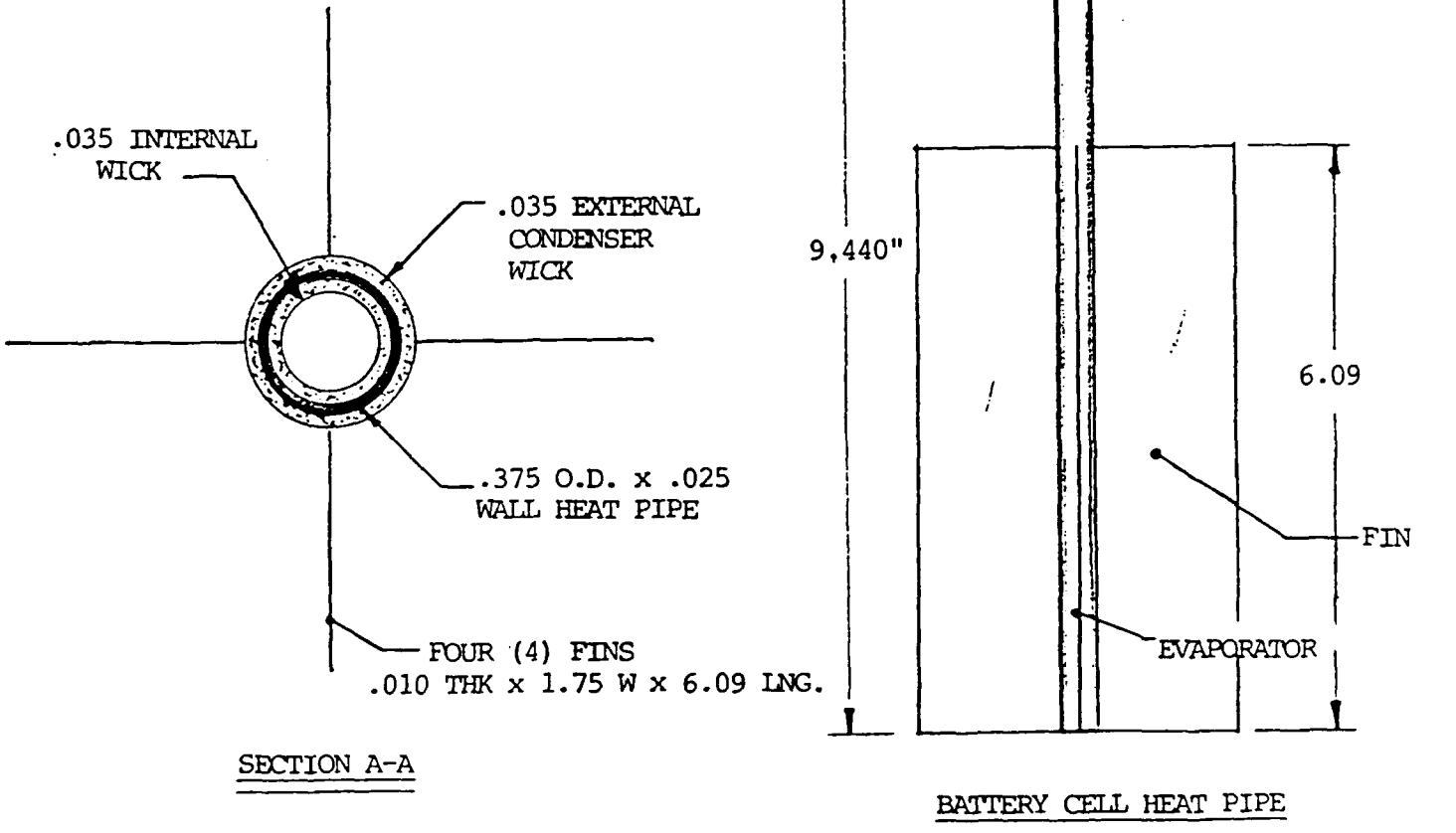

Figure 21. Battery cell heat pipe geometry

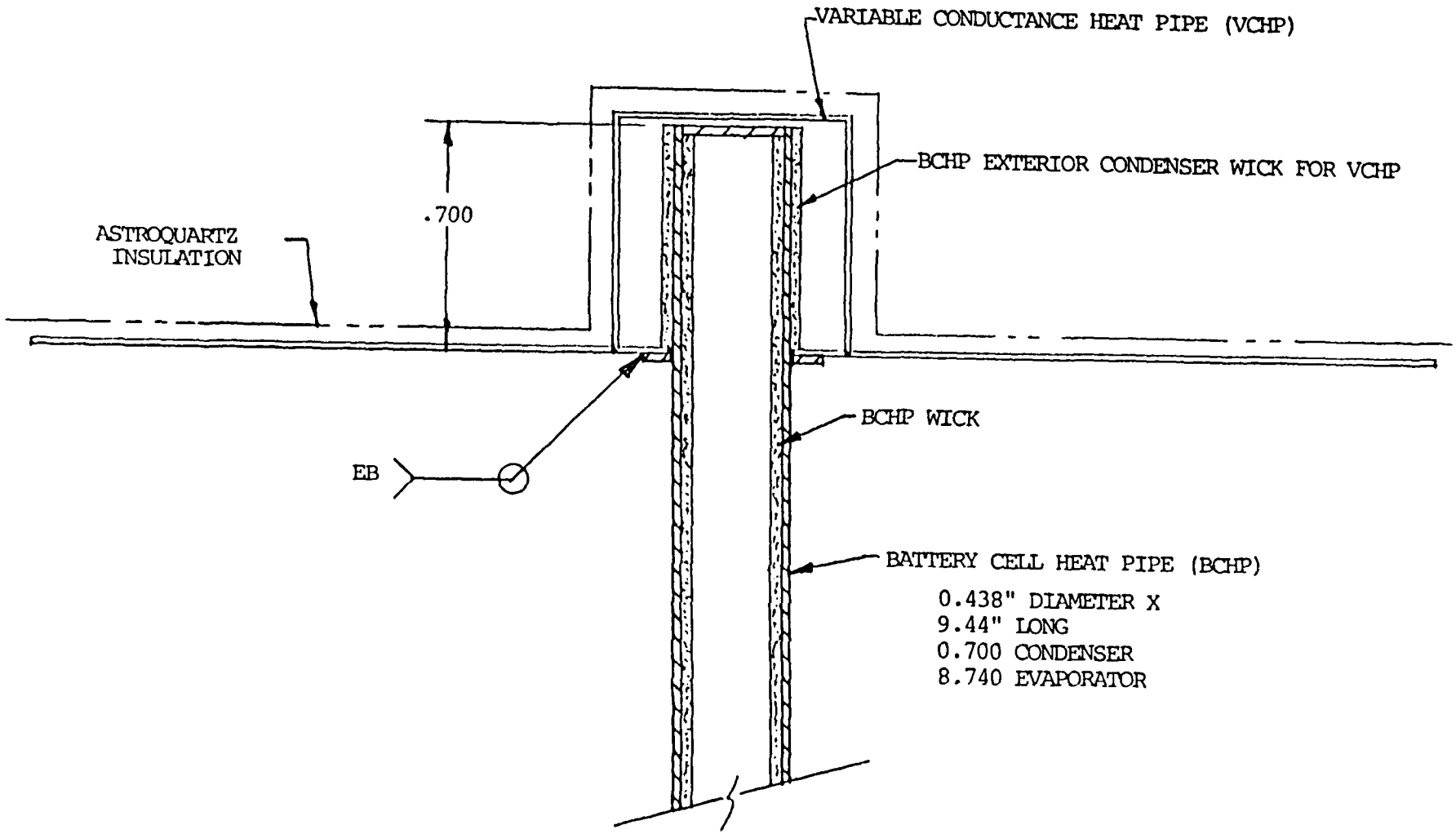

Figure 22. Battery cell heat pipe - VCHP assembly

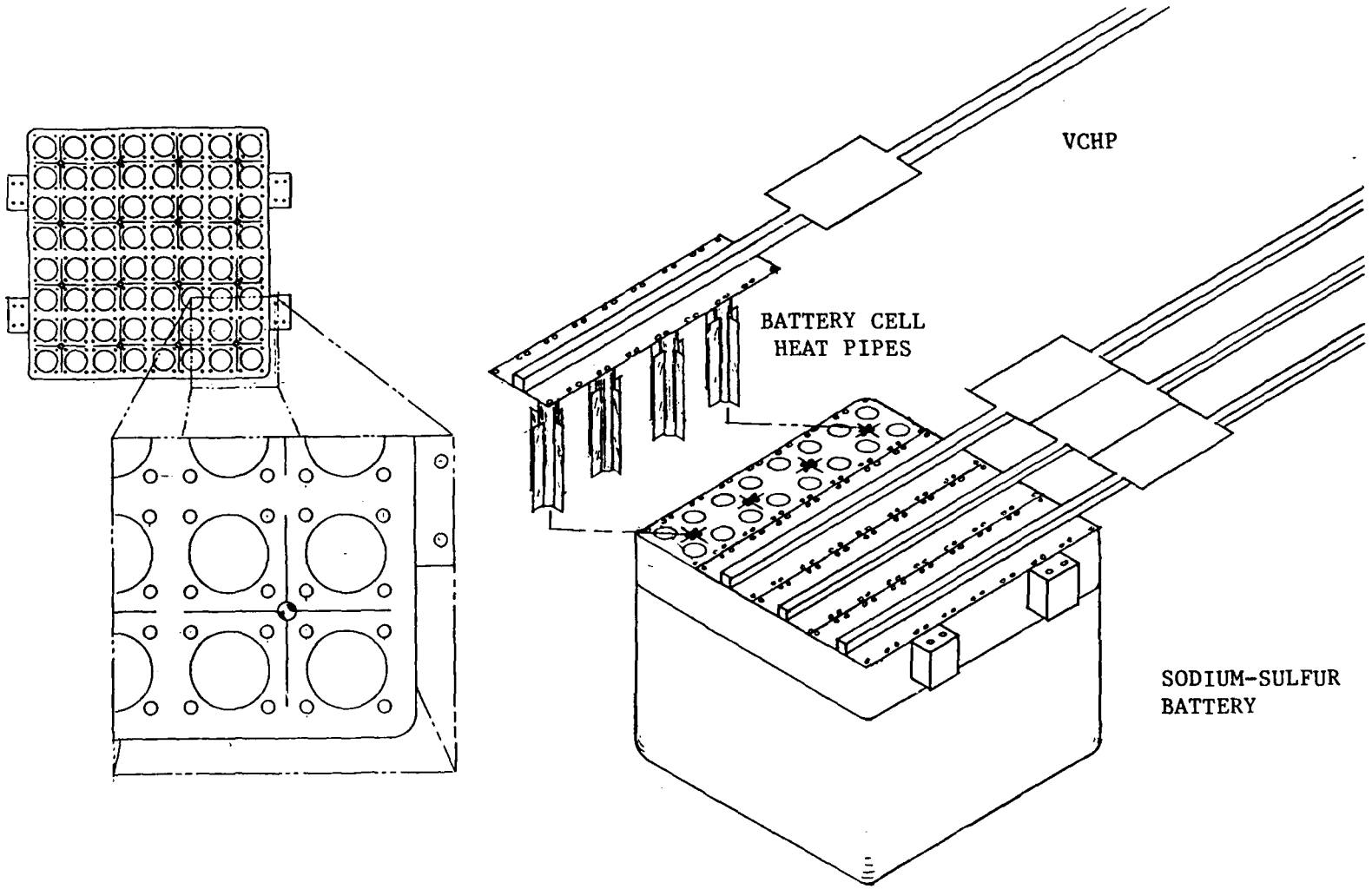

Figure 23. VCHP/BCHP integration with sodium-sulfur battery

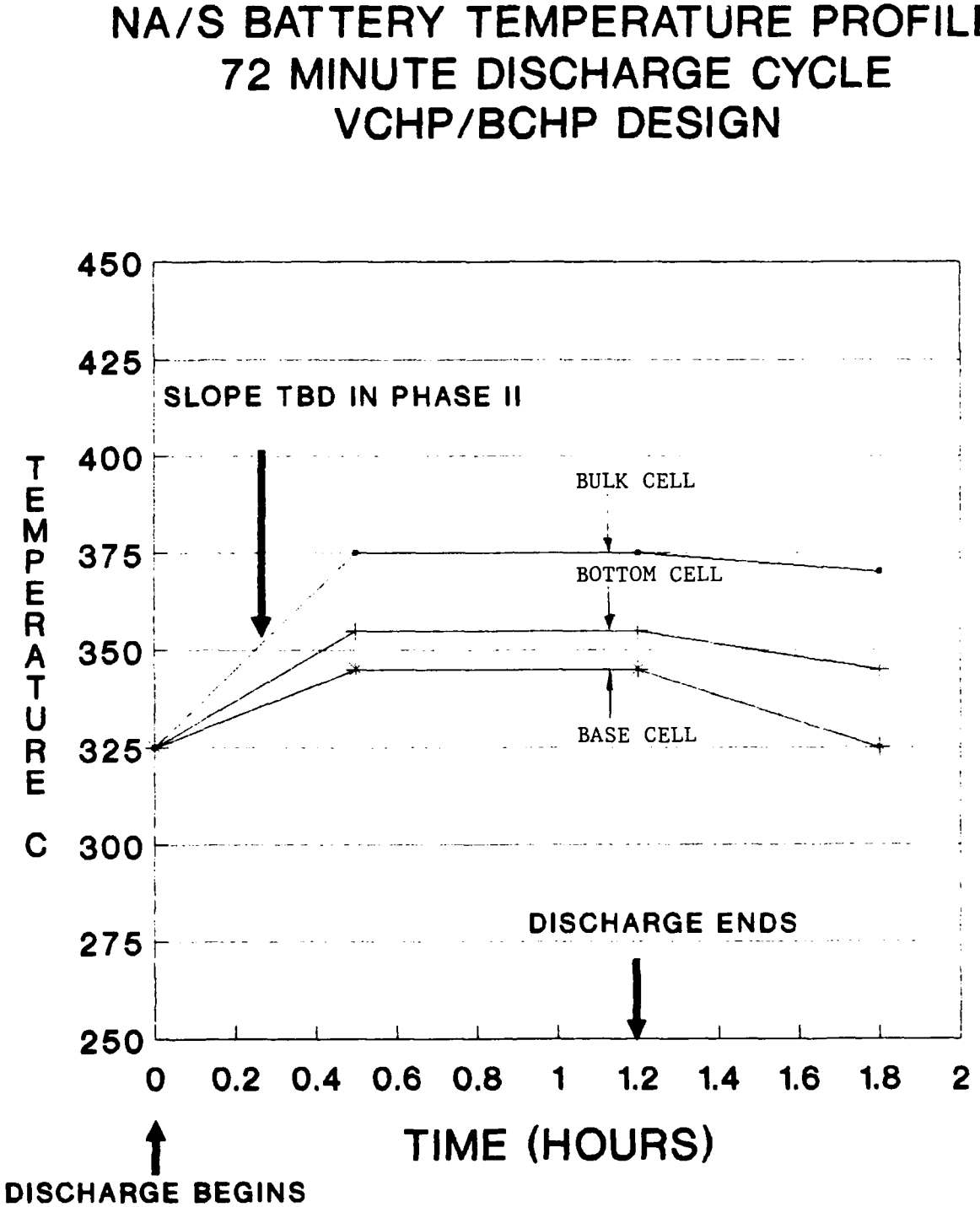

Figure 24. Na/S battery temperature profile - 72 minute discharge cycle - VCHP/BCHP design

The VCHP and base cell temperature will increase from 325°C to 345°C as the power in the battery increases from Q = 0 watts to Q = 500 watts. The bulk cell temperature will increase from 325°C to 375°C. In the analysis, the battery cells and BCHPs were coated with a high emissivity coating of 0.8 in order to enhance their radiative heat transfer properties. For the purpose of this preliminary analysis, it will be assumed that the bottom cell temperature is 355°C. The battery cell axial delta-T is therefore 20°C. A complete thermal analysis program will be written as part of a Phase II work effort.

3.4.3 Integration: Summary

A summary of the thermal analysis using VCHPs only and the dual heat pipe concept using VCHPs and BCHPs is shown in Table 3. Calculated thermal management weight for each design is also tabulated.

TABLE 3. VCHP Integration Summary

Thermal Management Design	Weight (lbs)	Battery Cell Axial Delta-T (°C) $T_{bulk} - T_{bottom}$	Bulk Cell Temperature (°C)
Louver	5.13	32	387
VCHP only	4.04	64	419*
VCHP w/BCHP	5.72	20	375

T_{bottom} = 355°C

*Peak cell temperature = 404°C

From the data presented, the VCHP design with BCHPs will provide a battery cell axial delta-T $\leq$ 20°C. This is an improvement over the louver concept which has a 32°C axial delta-T. The only disadvantage is the slight weight gain because of the addition of BCHPs.

APPENDIX A

VCHP Component and Assembly Drawings

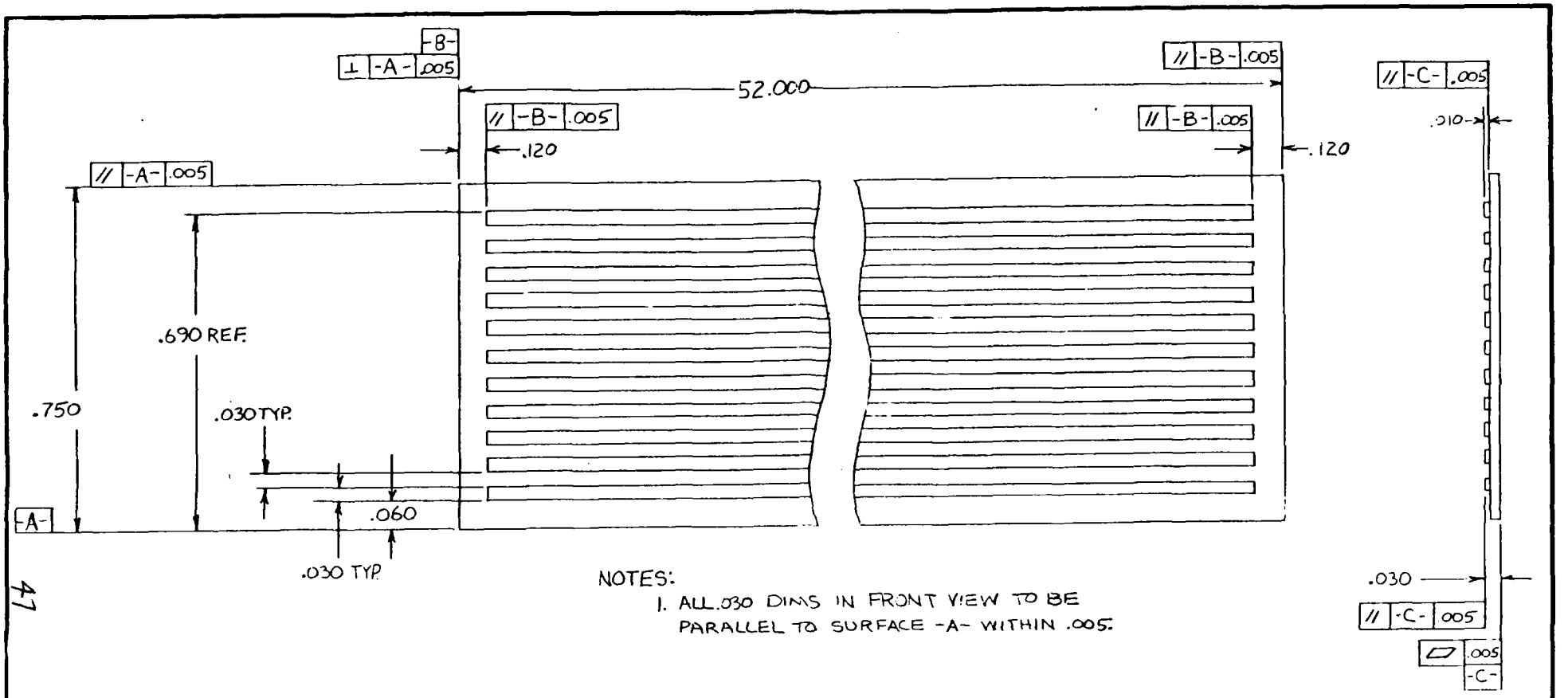

47

NOTES:

1. ALL .030 DIMS IN FRONT VIEW TO BE PARALLEL TO SURFACE -A- WITHIN .005.

MATL: TITANIUM CP GRADE 2

REVISIONS			
LTR.	DESCRIPTION	DATE	APPROVED
-A-	.120 WAS .060	1/17/89	JDH 1/18/89

UNLESS OTHERWISE SPECIFIED DIMENSIONS ARE IN INCHES
TOLERANCES
DECIMALS ANGULAR
.XX ± .010 ± .5°30'
.XXX ± .005
DO NOT SCALE DRAWING

TREATMENT

FINISH

SIMILAR TO | ACT. WT. | CALC. WT.

CONTRACT NO.

DRAWN DM — DATE 1/5/89

CHECK

APPROVED JDH R. Hunsaker — 1-12-89

APPROVED

CUSTOMER

THERMACORE, INC.
HEAT TRANSFER SPECIALISTS

TITLE: WICK STRUCTURE

SIZE B | DWG. NO. B-11-1030-1 | REV. A

SCALE 5X1 | RELEASE DATE | SHEET

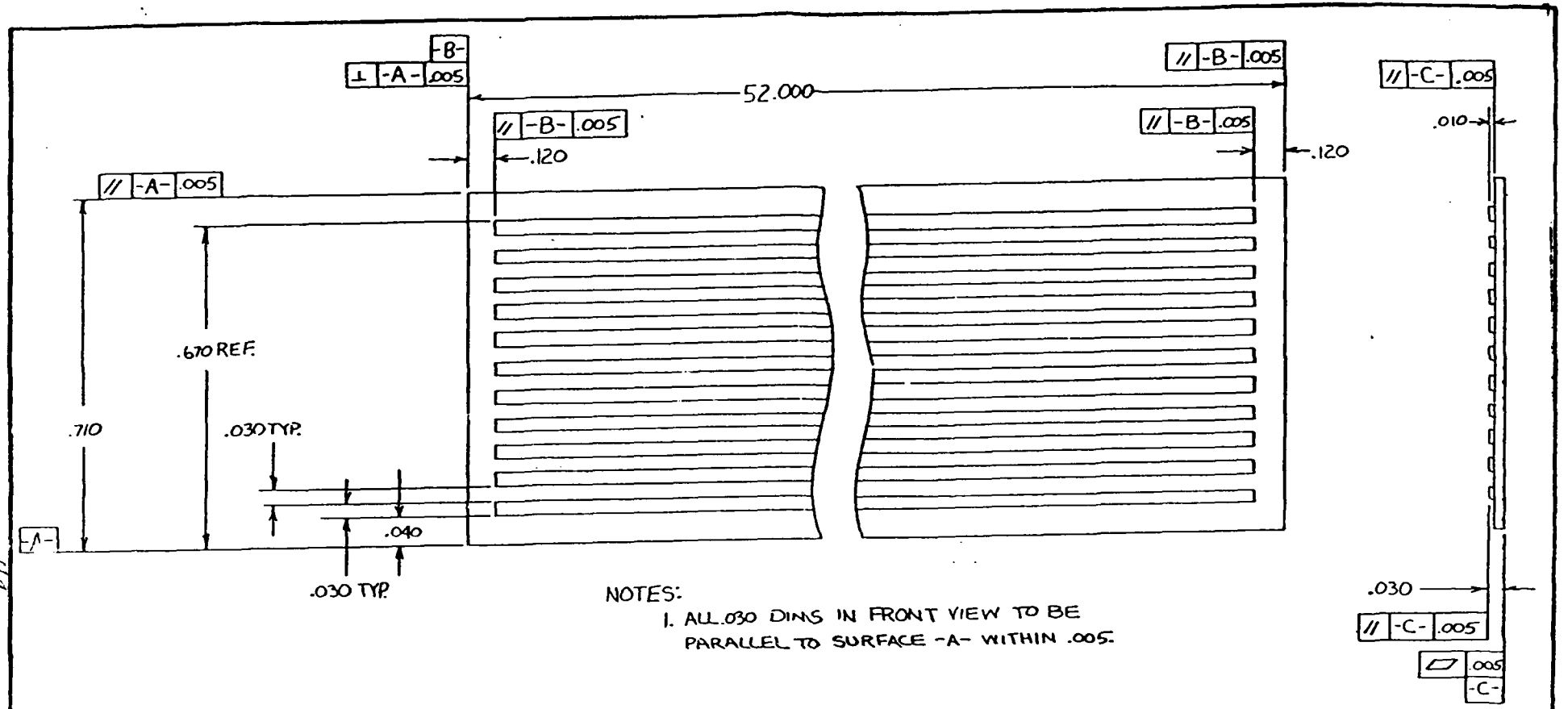

MATL: TITANIUM CP GRADE 2

REVISIONS			
LTR	DESCRIPTION	DATE	APPROVED
-A-	.120 WAS .060	1/17/89	JCH 1-18-89

UNLESS OTHERWISE SPECIFIED DIMENSIONS ARE IN INCHES TOLERANCES DECIMALS ANGULAR .xxx ± .010 ± .5° .xxxx ± .005 DO NOT SCALE DRAWING

TREATMENT

FINISH

SIMILAR TO | ACT. WT. | CALC. WT.

CONTRACT NO.

DRAWN DM DATE 1/5/89

CHECK

APPROVED John R. Antonetti 1-12-89

APPROVED

CUSTOMER

THERMACORE, INC.
HEAT TRANSFER SPECIALISTS

TITLE
WICK STRUCTURE

SIZE B | DWG. NO. B-11-1030-2 | REV A

SCALE 5X1 | RELEASE DATE | SHEET

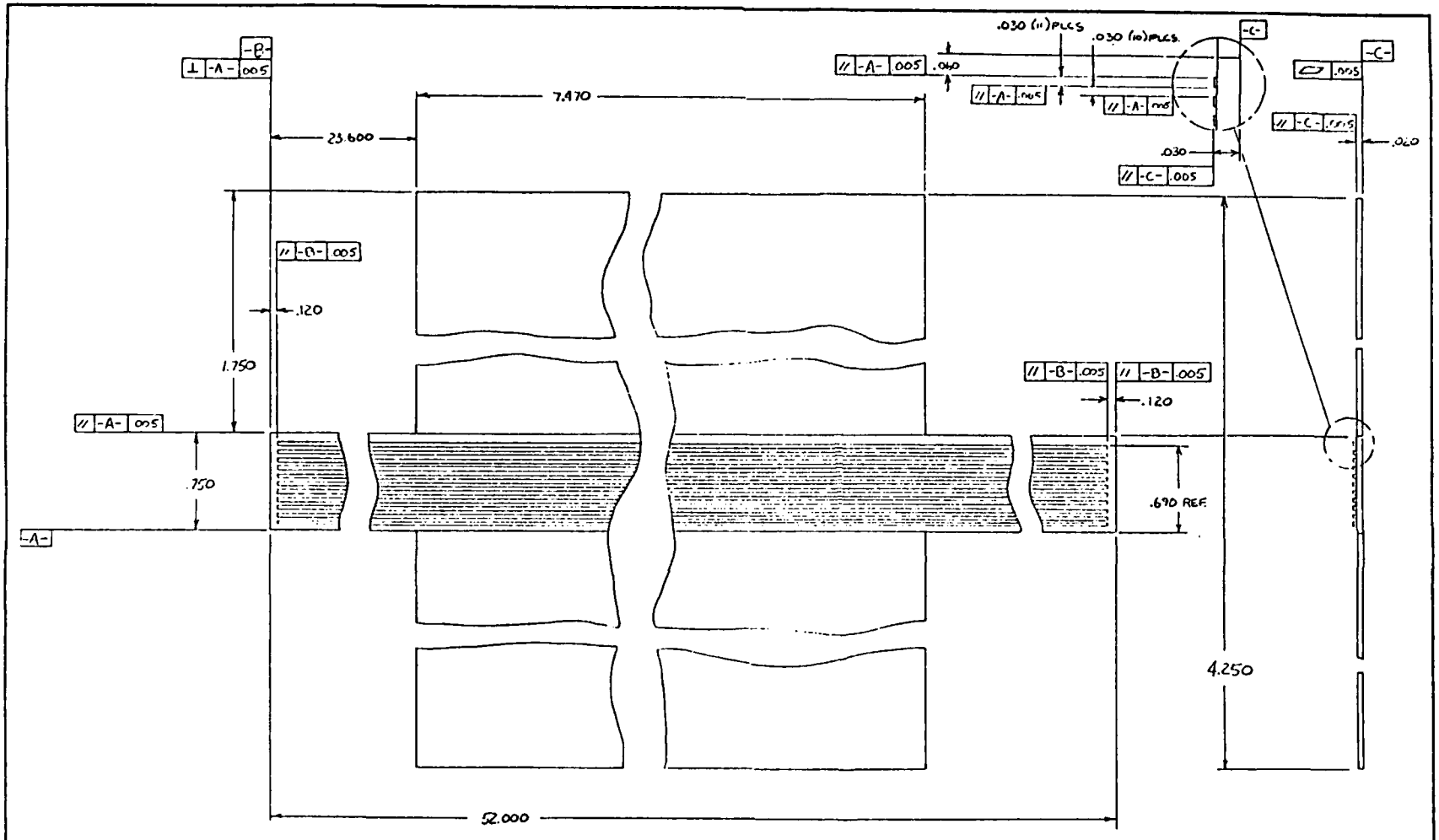

MATL: TITANIUM CP GRADE 2

REVISIONS			
LTR	DESCRIPTION	DATE	APPROVED
-A-	.120 WAS .060	12/17/89	JCH 12-18-89

DRAWN	DM	DATE 1/6/89
CHECK		
APPROVED	John P Hollingsworth	1-11-89
APPROVED		
CUSTOMER		

THERMACORE, INC.

TITLE: FIN STRUCTURE

SIZE C | DWG NO C-11-1030-3 | REV A

SCALE 2/1 | RELEASE DATE | SHEET

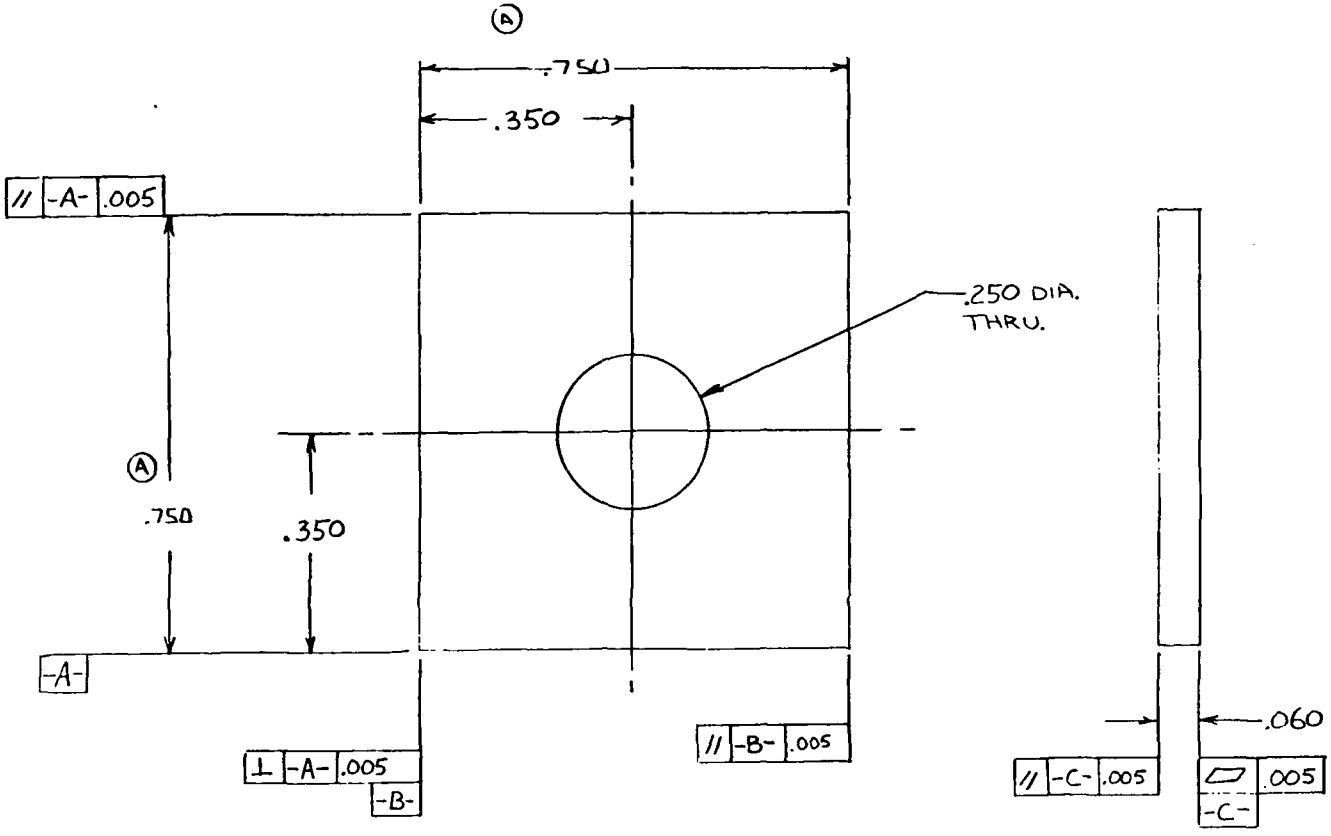

MATL: TITANIUM CP GRADE 2

UNLESS OTHERWISE SPECIFIED
DIMENSIONS ARE IN INCHES
TOLERANCES
DECIMALS ANGULAR
.XX ± .015 ± 0°30'
.XXX ± .005
DO NOT SCALE DRAWING

TREATMENT

FINISH

SIMILAR TO | ACT. WT. | CALC. WT.

CONTRACT NO.

		DATE
DRAWN	DM	1/6/89
CHECK		
APPROVED	John R. Hardester	1-12-89
APPROVED		
CUSTOMER		

THERMACORE, INC.
HEAT TRANSFER SPECIALISTS

TITLE
RESERVOIR END CAP

SIZE	DWG. NO.	REV
B	B-11-1030-4	A

SCALE 5 x 1 | RELEASE DATE | SHEET

REVISIONS

LTR.	DESCRIPTION	DATE	APPROVED
A	.750 W .705 +.000 -.002	1-23-89	EJD

QC

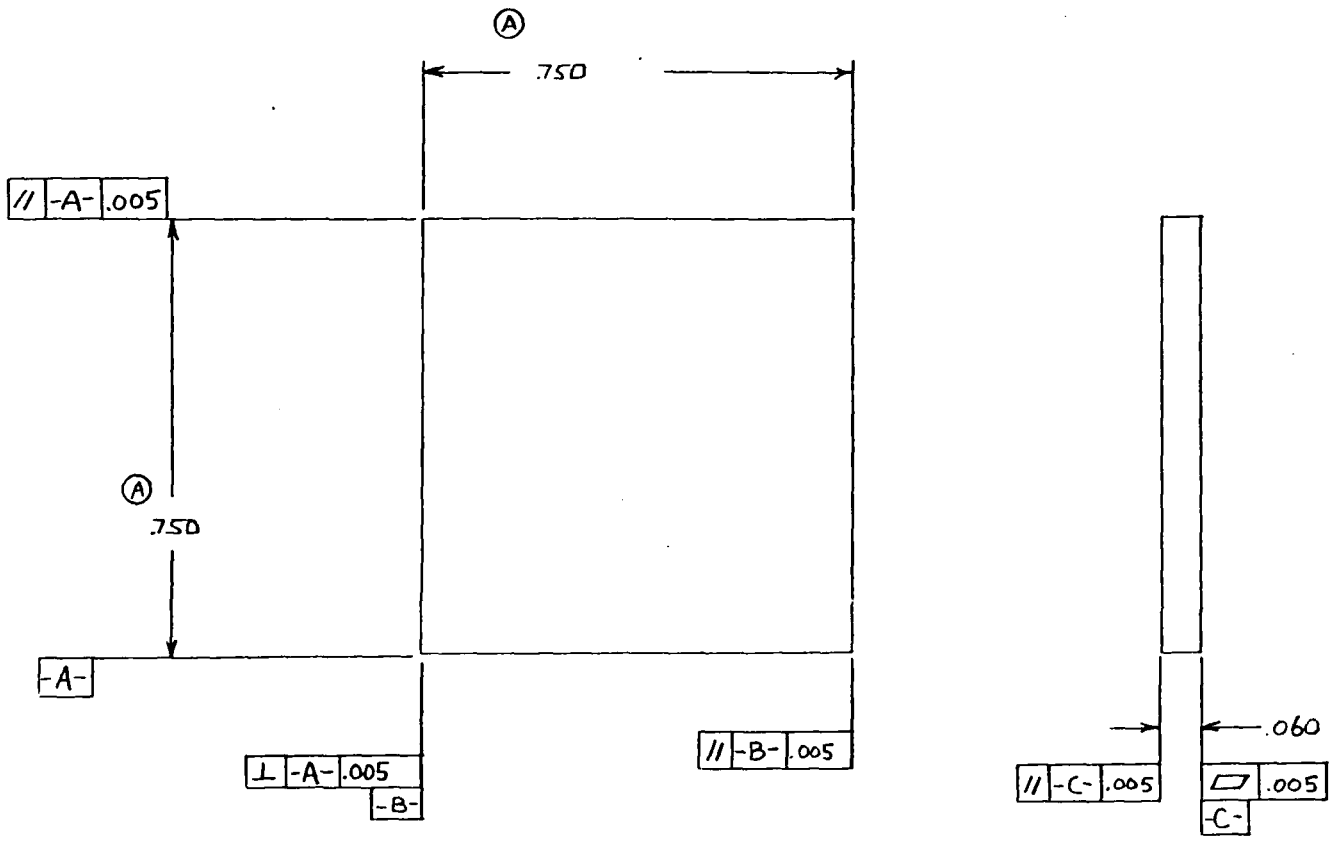

MATL: TITANIUM CP GRADE 2

REVISIONS			
LTR	DESCRIPTION	DATE	APPROVED
A	.750 W .705 +.000 -.002	1-23-89	EWD

UNLESS OTHERWISE SPECIFIED
DIMENSIONS ARE IN INCHES
TOLERANCES
DECIMALS ANGULAR
.XX ± .015 ± 0°30'
.XXX ± .005
DO NOT SCALE DRAWING

TREATMENT

FINISH

SIMILAR TO | ACT. WT. | CALC. WT.

CONTRACT NO.

DRAWN	DM	DATE 1/6/89
CHECK		
APPROVED	J. L. R. Hartantir	1-12-89
APPROVED		
CUSTOMER		

THERMACORE, INC.
HEAT TRANSFER SPECIALISTS

TITLE
EVAPORATOR END CAP

SIZE	DWG. NO.	REV
B	B-11-1030-5	A

SCALE 5x1 | RELEASE DATE | SHEET

15

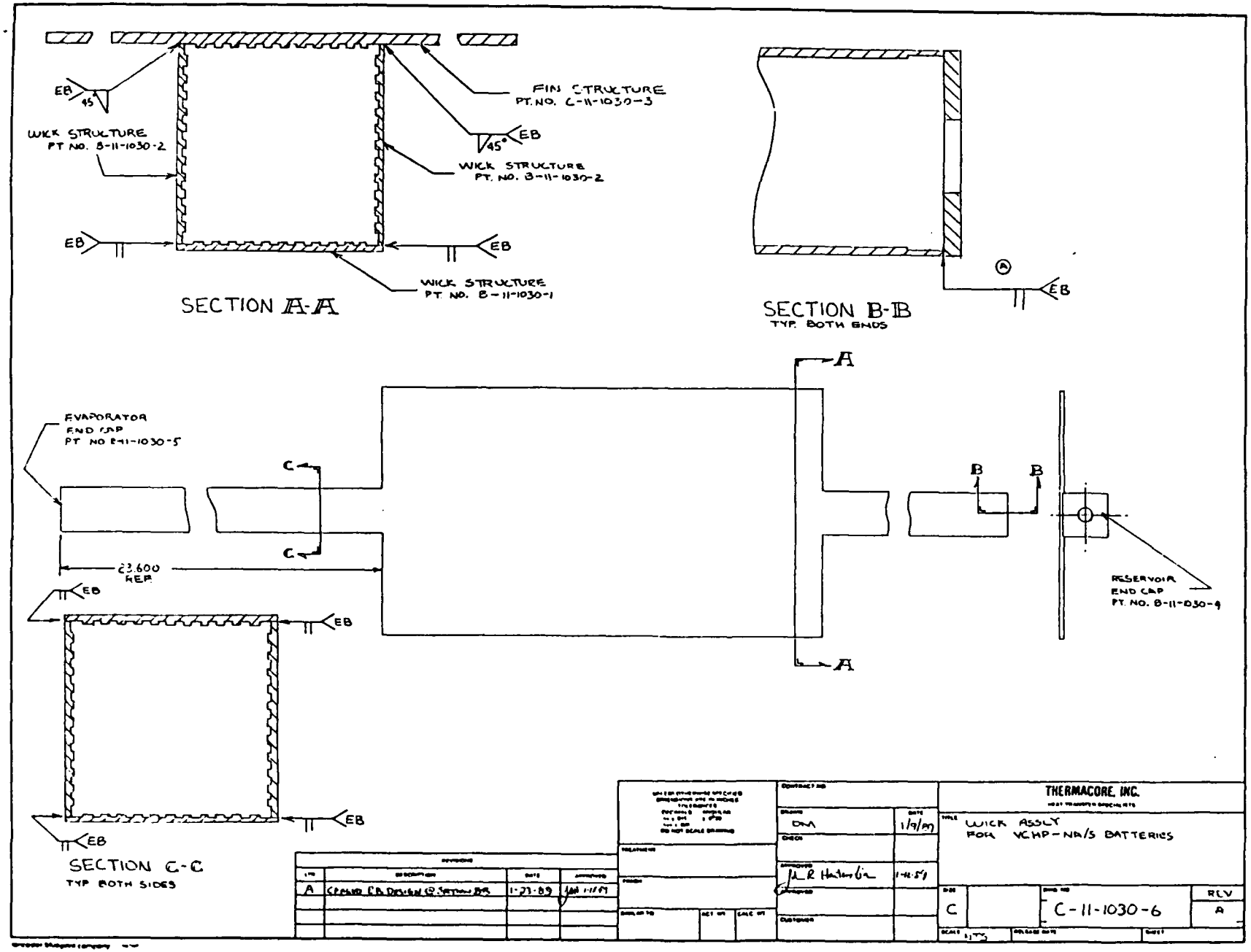

REV	DESCRIPTION	DATE	APPROVED
A	CHANGED C.B. DRAWING TO "BOTTOM" VIEW	1-23-89	1-19-89

DRAWN DM 1/9/89
CHECK
APPROVED L R Hallenbeck 1-16-89

THERMACORE, INC.

TITLE: WICK ASSLY FOR VCHP-NA/S BATTERIES

SIZE	DWG NO	REV
C	C-11-1030-6	A

SCALE 1:1 | RELEASE DATE | SHEET

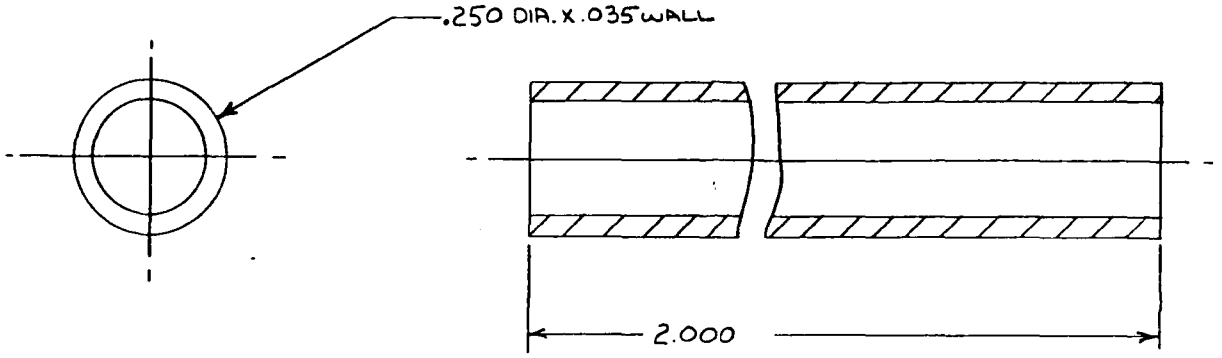

MATL: TITANIUM CP GRADE 2
SEAMLESS

REVISIONS			
LTR.	DESCRIPTION	DATE	APPROVED

UNLESS OTHERWISE SPECIFIED
DIMENSIONS ARE IN INCHES
TOLERANCES
DECIMALS ANGULAR
xx ± .015 ± 0°30'
xxx ± .005
DO NOT SCALE DRAWING

TREATMENT

FINISH

SIMILAR TO | ACT. WT. | CALC. WT.

CONTRACT NO.

DRAWN	Dm	DATE 1/10/89
CHECK		
APPROVED	J. R. Hartstine	1-12-89
APPROVED		
CUSTOMER		

THERMACORE, INC.
HEAT TRANSFER SPECIALISTS

TITLE: FILL TUBE

SIZE: B | DWG. NO.: B-11-1030-7

SCALE: 5 x 1 | RELEASE DATE | SHEET

63

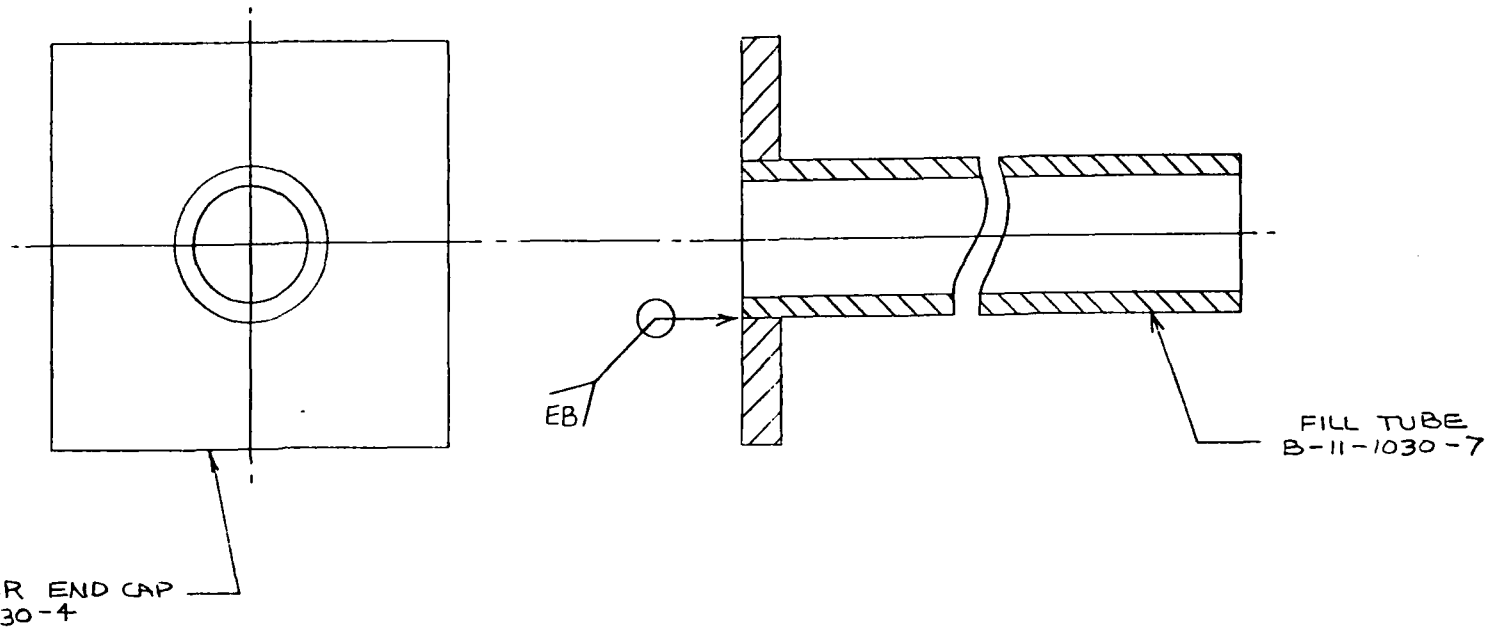

REVISIONS			
LTR.	DESCRIPTION	DATE	APPROVED

UNLESS OTHERWISE SPECIFIED
DIMENSIONS ARE IN INCHES
TOLERANCES
DECIMALS ANGULAR
.xx ± .015 ± 0°30'
.xxx ± .005
DO NOT SCALE DRAWING

TREATMENT

FINISH

SIMILAR TO | ACT WT. | CALC. WT.

CONTRACT NO.

		DATE
DRAWN	DM	1/10/89
CHECK		
APPROVED	John R Hankins	1-12-89
APPROVED		
CUSTOMER		

THERMACORE, INC.
HEAT TRANSFER SPECIALISTS

TITLE
WELD ASSLY
END CAP TO FILL TUBE

SIZE B | DWG NO. B-11-1030-8

SCALE 5X1 | RELEASE DATE | SHEET

APPENDIX B

Three-Dimensional Finite-Difference Program,
Diffusion Coefficient Calculation

```
CCCCCCCCCCCCCCCCCCCCCCCCCCCCCCCCCCCCCCCCCCCCCCCCCCCCCCCCCCCCCCCCCCCCCCCC
CCCCCCCCCC                    VCHP-RES                        CCCCCCCCCC
CCCCC                                                              CCCCC
CC         A FORTRAN PROGRAM WRITTEN BY JIM BOGART AT                 CC
CC                       THERMACORE, INC                              CC
CC                                                                    CC
CC  THIS PROGRAM DETERMINES THE CONCENTRATION DISTRIBUTION AND        CC
CC  TEMPERATURE DISTRIBUTION IN THE RESERVOIR OF A VARIABLE-          CC
CC  CONDUCTANCE HEAT PIPE.                                            CC
CC                                                                    CC
CCCCC                                                              CCCCC
CCCCCCCCCC                                                    CCCCCCCCCC
CCCCCCCCCCCCCCCCCCCCCCCCCCCCCCCCCCCCCCCCCCCCCCCCCCCCCCCCCCCCCCCCCCCCCCCC
C
C
      REAL*8 COND,DX,DX1,DY,DY1,DZ,D,EMISS,SIG,
     1TSINK,TS4,VHEAT,DISTZ
      INTEGER I,J,K,N,I1,J1,K1,FLAG
      REAL*8 T(10,10,20),C(10,10,20),OLDT(10,10,20),OLDC(10,10,20)
C
C----------------------------------------------------------------------C
C SET VALUES OF CONSTANT PARAMETERS AND NODAL SPACING
C----------------------------------------------------------------------C
C
      COND=21.9
      TSINK=273.
      VHEAT=5.4D05
      D=1.967D-03
      TS4=TSINK**4
      DX=1.4605D-03
      DX1=2.54D-04
      DY=DX
      DY1=DX1
      DZ=2.54D-02
      EMISS=0.6
      SIG=5.67D-08
C
C----------------------------------------------------------------------C
C INITIALIZE ALL VALUES OF TEMP & CONCENTRATION
C----------------------------------------------------------------------C
C
      DO 1 I=1,10
      DO 2 J=1,10
      DO 3 K=1,20
      T(I,J,K)=273.0
      C(I,J,K)=0.0
  3   CONTINUE
  2   CONTINUE
  1   CONTINUE
C
C---------------------------------------------------------------------C
C SET VALUES AT CONDENSER/RESERVOIR INTERFACE
C---------------------------------------------------------------------C
C
      DO 4 I=1,10
```

```
*     DO 5 J=1,10                                                    VCH00560
      T(I,J,1)=643.                                                  VCH00570
      C(I,J,1)=4.034E-02                                             VCH00580
   5  CONTINUE                                                       VCH00590
   4  CONTINUE                                                       VCH00600
C                                                                    VCH00610
C-------------------------------------------------------------------CVCH00620
C SAVE NEW TEMPERATURE AND CONCENTRATION VALUES TO A TEMPORARY MATRIX VCH00630
C TO COMPARE FOR CONVERGENCE OF THE CALCULATED VALUES FOR THE CURRENT VCH00640
C CALCULATION LOOP                                                   VCH00650
C-------------------------------------------------------------------CVCH00660
C                                                                    VCH00670
      FLAG=0                                                         VCH00680
  20  FLAG=FLAG+1                                                    VCH00690
      DO 21 I=1,10                                                   VCH00700
      DO 22 J=1,10                                                   VCH00710
      DO 23 K=1,20                                                   VCH00720
      OLDT(I,J,K)=T(I,J,K)                                           VCH00730
      OLDC(I,J,K)=C(I,J,K)                                           VCH00740
  23  CONTINUE                                                       VCH00750
  22  CONTINUE                                                       VCH00760
  21  CONTINUE                                                       VCH00770
      DO 6 K=2,19                                                    VCH00780
      DO 7 I=1,9                                                     VCH00790
*     DO 8 J=1,9                                                     VCH00800
C                                                                    VCH00810
C-------------------------------------------------------------------CVCH00820
C*SET TEMPERATURE GRADIENT AT THE FAR END OF THE RESERVOIR TO BE ZERO VCH00830
C-------------------------------------------------------------------CVCH00840
C                                                                    VCH00850
      IF(K.EQ.19)THEN                                                VCH00860
      T(I,J,20)=T(I,J,18)                                            VCH00870
      ENDIF                                                          VCH00880
C                                                                    VCH00890
C-------------------------------------------------------------------CVCH00900
C CALCULATE SOME CONVENIENCE PARAMETERS                              VCH00910
C-------------------------------------------------------------------CVCH00920
C                                                                    VCH00930
      I1=I+1                                                         VCH00940
      I1N=I-1                                                        VCH00950
      I2=I+2                                                         VCH00960
      J2=J+2                                                         VCH00970
      J1=J+1                                                         VCH00980
      J1N=J-1                                                        VCH00990
      I2N=I-2                                                        VCH01000
      J2N=J-2                                                        VCH01010
      K1=K+1                                                         VCH01020
      K1N=K-1                                                        VCH01030
C                                                                    VCH01040
C-------------------------------------------------------------------CVCH01050
C OUTSIDE CORNER NODE                                                VCH01060
C-------------------------------------------------------------------CVCH01070
C                                                                    VCH01080
      IF(I.EQ.1.AND.J.EQ.1) THEN                                     VCH01090
      T(I,J,K)=((T(I,J1,K)+T(I1,J,K))/DX1**2-EMISS*SIG/COND/DX1*2*(T(I,JVCH01100
```

```
     1,K)**4-TS4)+(T(I,J,K1)+T(I,J,K1N))/DZ**2)/(DX1**(-2)+DZ**(-2))/2  VCH01110
      ENDIF                                                             VCH01120
C      -'                                                               VCH01130
C-----------------------------------------------------------------------CVCH01140
C WALL NODES - OUTSIDE, LEFT FACE                                       VCH01150
C-----------------------------------------------------------------------CVCH01160
C                                                                       VCH01170
      IF(I.EQ.1.AND.J.EQ.2)THEN                                         VCH01180
      T(I,J,K)=((T(1,3,K)+T(1,1,K))/DY1**2+(T(1,2,K1)+T(1,2,K1N))/DZ**2+VCH01190
     1T(2,2,K)/DX1**2-EMISS*SIG/COND/DX1*(T(I,J,K)**4-TS4))/(2/DY1**2+1/VCH01200
     1DX1**2+2/DZ**2)                                                   VCH01210
      ENDIF                                                             VCH01220
      IF(I.EQ.1.AND.J.EQ.3)THEN                                         VCH01230
      T(I,J,K)=(T(1,2,K)/DY1**2+2*T(1,4,K)/(DY1+DY)/DY1+T(2,3,K)/DX1**2+VCH01240
     1(T(1,3,K1)+T(1,3,K1N))/DZ**2-EMISS*SIG/COND/DX1*(T(I,J,K)**4-TS4))VCH01250
     1/(1/DY1**2+2/(DY+DY1)/DY1+1/DX1**2+2/DZ**2)                       VCH01260
      ENDIF                                                             VCH01270
      IF(I.EQ.1.AND.J.EQ.4)THEN                                         VCH01280
      T(I,J,K)=(T(2,4,K)/DX1**2+2*T(1,3,K)/(DY1+DY)/DY+T(1,5,K)/DY/DY+(TVCH01290
     1(1,4,K1                                                           VCH01300
     1)+T(1,4,K1N))/DZ**2-EMISS*SIG/COND/DY1*(T(1,4,K)**4-TS4))/(1/DX1**VCH01310
     12+2/(DY+DY1)/DY+1/DY/DY+2/DZ**2)                                  VCH01320
      ENDIF                                                             VCH01330
      IF(I.EQ.1.AND.J.GT.4)THEN                                         VCH01340
      T(I,J,K)=1/(1/DX1**2+2/DY**2+2/DZ**2)*(T(I1,J,K)/DX1**2-EMISS*    VCH01350
     1SIG/COND/DY1*(T(1,J,K)**4-TS4)+(T(I,J1,K)+T(I,J1N,K))/DY**2+(T(I, VCH01360
     1J,K1)+T(I,J,K1N))/DZ**2)                                          VCH01370
      T(1,10,K)=T(1,6,K)                                                VCH01380
      ENDIF                                                             VCH01390
C                                                                       VCH01400
C-----------------------------------------------------------------------CVCH01410
C WALL NODES - OUTSIDE, BOTTOM FACE                                     VCH01420
C-----------------------------------------------------------------------CVCH01430
C                                                                       VCH01440
      IF(I.EQ.2.AND.J.EQ.1)THEN                                         VCH01450
      T(I,J,K)=((T(3,1,K)+T(1,1,K))/DX1**2+(T(2,1,K1)+T(2,1,K1N))/DZ**2+VCH01460
     1T(2,2,K)/DY1**2-EMISS*SIG/COND/DY1*(T(I,J,K)**4-TS4))/(2/DX1**2+1/VCH01470
     1DY1**2+2/DZ**2)                                                   VCH01480
      ENDIF                                                             VCH01490
      IF(I.EQ.3.AND.J.EQ.1)THEN                                         VCH01500
      T(I,J,K)=(T(2,1,K)/DX1**2+2*T(4,1,K)/(DX1+DX)/DX1+T(3,2,K)/DY1**2+VCH01510
     1(T(3,1,K1)+T(3,1,K1N))/DZ**2-EMISS*SIG/COND/DY1*(T(I,J,K)**4-TS4))VCH01520
     1/(1/DX1**2+2/(DX+DX1)/DX1+1/DY1**2+2/DZ**2)                       VCH01530
      ENDIF                                                             VCH01540
      IF(I.EQ.4.AND.J.EQ.1)THEN                                         VCH01550
      T(I,J,K)=(T(4,2,K)/DY1**2+2*T(3,1,K)/(DX1+DX)/DX+T(5,1,K)/DX/DX+(TVCH01560
     1(4,1,K1                                                           VCH01570
     1)+T(4,1,K1N))/DZ**2-EMISS*SIG/COND/DY1*(T(4,1,K)**4-TS4))/(1/DY1**VCH01580
     12+2/(DX+DX1)/DX+1/DX/DX+2/DZ**2)                                  VCH01590
      ENDIF                                                             VCH01600
      IF(I.GT.4.AND.J.EQ.1)THEN                                         VCH01610
      T(I,J,K)=1/(1/DY1**2+2/DX**2+2/DZ**2)*(T(I,J1,K)/DY1**2-EMISS*    VCH01620
     1SIG/COND/DY1*(T(I,J,K)**4-TS4)+(T(I1,J,K)+T(I1N,J,K))/DX**2+(T(I, VCH01630
     1J,K1)+T(I,J,K1N))/DZ**2)                                          VCH01640
      T(10,1,K)=T(8,1,K)                                                VCH01650
```

```
      ENDIF                                                                 VCH01660
C                                                                           VCH01670
C-------------------------------------------------------------------------CVCH01680
C WALL NODES - INSIDE CORNER & MIDDLE CORNER                                VCH01690
C-------------------------------------------------------------------------CVCH01700
C                                                                           VCH01710
      IF(I.EQ.2.AND.J.EQ.2)THEN                                             VCH01720
      T(I,J,K)=0.5/(DX1**(-2)+DY1**(-2)+DZ**(-2))*((T(I1,J,K)+T(I1N,J,K)VCH01730
     1)/DX1                                                                 VCH01740
     1**2+(T(I,J1,K)+T(I,J1N,K))/DY1**2+(T(I,J,K1)+T(I,J,K1N))/DZ**2)       VCH01750
      ENDIF                                                                 VCH01760
      IF(I.EQ.2.AND.J.EQ.3)THEN                                             VCH01770
      T(I,J,K)=((T(I,J,K1)+T(I,J,K1N))/DZ**2+(T(I1,J,K)+T(I1N,J,K))/DX1 VCH01780
     1**2+T(I,J1N,K)/DY1**2+2*T(I,J1,K)/(DY+DY1)/DY1)/(2/DZ**2+2/DX1**2+VCH01790
     11/DY1**2+2/(DY+DY1)/DY1)                                              VCH01800
      ENDIF                                                                 VCH01810
      IF(I.EQ.3.AND.J.EQ.2)THEN                                             VCH01820
      T(I,J,K)=((T(I,J,K1)+T(I,J,K1N))/DZ**2+(T(I,J1,K)+T(I,J1N,K))/DY1 VCH01830
     1**2+T(I1N,J,K)/DX1**2+2*T(I1,J,K)/(DX+DX1)/DX1)/(2/DZ**2+2/DY1**2+VCH01840
     11/DX1**2+2/(DX+DX1)/DX1)                                              VCH01850
      ENDIF                                                                 VCH01860
      IF(I.EQ.3.AND.J.EQ.3)THEN                                             VCH01870
      T(I,J,K)=((T(I,J,K1)+T(I,J,K1N))/DZ**2+T(I,J1N,K)/DY1**2+2*T(I,J1,VCH01880
     1K)/(DY+DY1),/DY1+T(I1N,J,K),/DX1**2+2*T(I1,J,K)/(DX+DX1)/DX1)/(2/DZ VCH01890
     1**2+1/DX1**2+1/DY1**2+4/(DX+DX1)/DX1)                                 VCH01900
      ENDIF                                                                 VCH01910
C                                                                           VCH01920
C-------------------------------------------------------------------------CVCH01930
C WALL NODES - INSIDE, LEFT FACE                                            VCH01940
C-------------------------------------------------------------------------CVCH01950
C                                                                           VCH01960
  51  IF(I.EQ.2.AND.J.EQ.4)THEN                                             VCH01970
      T(I,J,K)=(T(I,J1N,K)/(DY+DY1),/DY**2+T(I,J1,K)/DY/DY+(T(I1,J,K)+      VCH01980
     1T(I1N,                                                                VCH01990
     1J,K))/DX1**2+(T(I,J,K1)+T(I,J,K1N))/DZ**2)/(2/DX1**2+2/(DY+DY1)/DYVCH02000
     1+1/DY**2+2/DZ**2)                                                     VCH02010
      ENDIF                                                                 VCH02020
      IF(I.EQ.2.AND.J.GT.4)THEN                                             VCH02030
      T(I,J,K)=0.5/(DX1**(-2)+DY**(-2)+DZ**(-2))*((T(I1,J,K)+T(I1N,J,K))VCH02040
     1/DX1                                                                  VCH02050
     1**2+(T(I,J1,K)+T(I,J1N,K))/DY**2+(T(I,J,K1)+T(I,J,K1N))/DZ**2)        VCH02060
      T(2,10,K)=T(2,8,K)                                                    VCH02070
      ENDIF                                                                 VCH02080
C                                                                           VCH02090
C-------------------------------------------------------------------------CVCH02100
C WALL NODES - INSIDE, BOTTOM FACE                                          VCH02110
C-------------------------------------------------------------------------CVCH02120
C                                                                           VCH02130
      IF(I.EQ.4.AND.J.EQ.2)THEN                                             VCH02140
      T(I,J,K)=(T(I1N,J,K)/(DX+DX1),/DX**2+T(I1,J,K)/DX/DX+(T(I,J1,K)+      VCH02150
     1T(I,J1                                                                VCH02160
     1N,K))/DY1**2+(T(I,J,K1)+T(I,J,K1N))/DZ**2)/(2/DY1**2+2/(DX+DX1)/DXVCH02170
     1+1/DX**2+2/DZ**2)                                                     VCH02180
      ENDIF                                                                 VCH02190
      IF(I.GT.4.AND.J.EQ.2)THEN                                             VCH02200
```

```
      T(I,J,K)=0.5/(DX**(-2)+DY1**(-2)+DZ**(-2))*((T(I1,J,K)+T(I1N,J,K))/DX VCH02210
     1**2+(T(I,J1,K)+T(I,J1N,K))/DY1**2+(T(I,J,K1)+T(I,J,K1N))/DZ**2)      VCH02220
      T(10,2,K)=T(8,2,K)                                                   VCH02230
      ENDIF                                                                VCH02240
      ENDIF                                                                VCH02250
C                                                                          VCH02260
C-------------------------------------------------------------------------CVCH02270
C WALL NODES - ADJACENT TO VAPOR CORE, LEFT FACE                           VCH02280
C-------------------------------------------------------------------------CVCH02290
C                                                                          VCH02300
      IF(I.EQ.3.AND.J.GT.3)THEN                                            VCH02310
      T(I,J,K)=T(I1N,J,K)+D*VHEAT/COND/DX*DX1*(C(I2,J,K)-C(I1,J,K))        VCH02320
      T(3,10,K)=T(3,8,K)                                                   VCH02330
      ENDIF                                                                VCH02340
C                                                                          VCH02350
C-------------------------------------------------------------------------CVCH02360
C WALL NODES - ADJACENT TO VAPOR CORE, BOTTOM FACE                         VCH02370
C-------------------------------------------------------------------------CVCH02380
C                                                                          VCH02390
      IF(I.GT.3.AND.J.EQ.3)THEN                                            VCH02400
      T(I,J,K)=T(I,J1N,K)+D*VHEAT/COND/DY*DY1*(C(I,J2,K)-C(I,J1,K))        VCH02410
      T(10,3,K)=T(8,3,K)                                                   VCH02420
      ENDIF                                                                VCH02430
C                                                                          VCH02440
C-------------------------------------------------------------------------CVCH02450
C VAPOR NODES - NEAR LEFT WALL                                             VCH02460
C-------------------------------------------------------------------------CVCH02470
C                                                                          VCH02480
      IF(I.EQ.4.AND.J.GT.3)THEN                                            VCH02490
      C(I,J,K)=C(I1,J,K)+COND*DX/D/VHEAT/DX1*(T(I2N,J,K)-T(I1N,J,K))       VCH02500
      C(4,10,K)=C(4,8,K)                                                   VCH02510
      ENDIF                                                                VCH02520
C                                                                          VCH02530
C-------------------------------------------------------------------------CVCH02540
C VAPOR NODES - NEAR BOTTOM WALL                                           VCH02550
C-------------------------------------------------------------------------CVCH02560
C                                                                          VCH02570
      IF(I.GT.3.AND.J.EQ.4)THEN                                            VCH02580
      C(I,J,K)=C(I,J1,K)+COND*DY/D/VHEAT/DY1*(T(I,J2N,K)-T(I,J1N,K))       VCH02590
      C(10,4,K)=C(8,4,K)                                                   VCH02600
      ENDIF                                                                VCH02610
C                                                                          VCH02620
C-------------------------------------------------------------------------CVCH02630
C VAPOR NODES - CORE                                                       VCH02640
C-------------------------------------------------------------------------CVCH02650
C                                                                          VCH02660
      IF(I.GT.4.AND.J.GT.4)THEN                                            VCH02670
      C(I,J,K)=(C(I1,J,K)+C(I1N,J,K)+C(I,J1,K)+C(I,J1N,K)+C(I,J,K1)+       VCH02680
     1C(I,J,K1N))/6                                                        VCH02690
      C(I,10,K)=C(I,8,K)                                                   VCH02700
      C(10,J,K)=C(8,J,K)                                                   VCH02710
      ENDIF                                                                VCH02720
 8    CONTINUE                                                             VCH02730
 7    CONTINUE                                                             VCH02740
 6    CONTINUE                                                             VCH02750
```

```
C      IF(FLAG.EQ.650)THEN                                              VCH02760
C      WRITE(*,1010)FLAG                                                VCH02770
 1010 FORMAT(/,I5,//)                                                   VCH02780
C      GOTO 1000                                                        VCH02790
C      ENDIF                                                            VCH02800
C                                                                       VCH02810
C-----------------------------------------------------------------------CVCH02820
C CONVERGENCE CHECK                                                     VCH02830
C-----------------------------------------------------------------------CVCH02840
C                                                                       VCH02850
       DO 30 I=1,9                                                      VCH02860
       DO 31 J=1,9                                                      VCH02870
       DO 32 K=2,19                                                     VCH02880
       IF(DABS(T(I,J,K)-OLDT(I,J,K)).GT.0.05)GOTO 20                    VCH02890
       IF(DABS(C(I,J,K)-OLDC(I,J,K)).GT.1D-04)GOTO 20                   VCH02900
  32   CONTINUE                                                         VCH02910
  31   CONTINUE                                                         VCH02920
  30   CONTINUE                                                         VCH02930
C                                                                       VCH02940
C-----------------------------------------------------------------------CVCH02950
C PRINTING SECTION                                                      VCH02960
C-----------------------------------------------------------------------CVCH02970
C                                                                       VCH02980
      WRITE(*,1010)FLAG                                                 VCH02990
 1000 DO 40 K=1,20                                                      VCH03000
       DISTZ=K*DZ/2.54D-02-DZ/2.54D-02                                  VCH03010
      WRITE(*,100)DISTZ                                                 VCH03020
  100  FORMAT(/,'Z-LOCATION =',2X,F6.3,1X,'INCHES',//)                  VCH03030
       DO 41 N=2,10                                                     VCH03040
       J=11-N                                                           VCH03050
       WRITE(*,101)(T(I,J,K),I=1,9)                                     VCH03060
  101  FORMAT(1X,10(1PE8.2,2X))                                         VCH03070
   41  CONTINUE                                                         VCH03080
       WRITE(*,2000)                                                    VCH03090
 2000 FORMAT(' ',///)                                                   VCH03100
       DO 42 N=2,10                                                     VCH03110
       J=11-N                                                           VCH03120
       WRITE(*,102)(C(I,J,K),I=1,10)                                    VCH03130
  102  FORMAT(1X,10(F11.9,1X))                                          VCH03140
   42  CONTINUE                                                         VCH03150
   40  CONTINUE                                                         VCH03160
       STOP                                                             VCH03170
       END                                                              VCH03180
                                                                        VCH03190
                                                                        VCH03200
```

Title: _____
Calculated by: H Bryant Date: 1/12/89
Checked by: _____ Date: _____
Reviewed by: _____ Date: _____
Project: 11-1030 Nals Battery
Page 13 of _____

Estimation of the diffusion coefficient of Cs in Ar

Ref: Perry & Chilton, Chemical Engineers' Handbook, 5th edition, pg (3-230)-(3-235)

eqn. (3-29) - Wilke-Lee modification of Hirschfelder, Bird, & Spotz eqn

$$D_G = \frac{B\,T^{3/2}\sqrt{(1/M_1)+(1/M_2)}}{P\,r_{12}^2\,I_D}$$

where D_G = gas diffusivity, [cm^2/s]

$$B = \left(10.85 - 250\sqrt{(\tfrac{1}{M_1})+(\tfrac{1}{M_2})}\right)\times 10^{-4}$$
$$= \left(10.85 - 250\left[\tfrac{1}{132.91}+\tfrac{1}{39.95}\right]^{1/2}\right)\times 10^{-4}$$
$$= 1.040\times 10^{-3}$$

T = absolute temperature [K]

M_1, M_2 = molecular weights of components 1 & 2

P = absolute pressure, atm

r_{12} = collision diameter [Å]
$= [(r_o)_1 + (r_o)_2]/2$

$r_o = 1.18\,V_b^{1/3}$

V_b = Hold volume of liquid @ normal boiling pt [cm^3/g-mole]

I_D = collision integral for diffusion

Title: _____ Calculated by: J. Bogart Date: 1/12/84
Checked by: _____ Date: _____
Reviewed by: _____ Date: _____
Project: 11-1030 Na/S Battery
Page 14 of _____

Calculate @ 370°C (643 K):

$P = 1520.2\ N/m^2 = 1520.2\ Pa = \frac{1520.2\ Pa}{101,300\ Pa/atm} = 0.015\ atm$

for argon: $r_{o_{A_r}} = 3.418\ \text{Å}$ (Table 3-308, Perry)

$(\epsilon/k)_{A_r} = 124.0\ K$

for cesium: $M_{Cs} = 132.91\ g/g\text{-mol}$

$\rho_{Cs\ @\ 1atm} = 1472\ kg/m^3 = 1.472\ g/cm^3$

$V_{bCs} = \frac{M_{Cs}}{\rho_{Cs}} = \frac{132.91\ g/g\text{-mol}}{1.472\ g/cm^3} = 90.292\ cm^3/g\text{-mol}$

$r_{o_{Cs}} = 1.18\ V_b^{1/3} = 5.159\ \text{Å}$

$(\epsilon/k)_{Cs} = 1.15\ T_b = 1.15(942.3\ K) = 1083.645\ K$

eqn. (3-29d): $\frac{\epsilon_{12}}{k} = \left[\left(\frac{\epsilon}{k}\right)_{Cs} * \left(\frac{\epsilon}{k}\right)_{A_r}\right]^{1/2} = [(1083.645)(124.0)]^{1/2}$

$\frac{\epsilon_{12}}{k} = 366.57$

Collision integral: $\left(\frac{k}{\epsilon_{12}}\right)(643\ K) = \frac{643}{366.57} = 1.754$ (643 K: operating temp.)

use Table (3-30f) of Perry and linearly interpolate:

$I_D = 0.5626$

Title: _____ Calculated by: A. Cagnato Date: 1/12/89
Checked by: _____ Date: _____
Reviewed by: _____ Date: _____
Project: 11-1020 Na/S Battery
Page 15 of _____

Calculate collision diameter:

$$r_{12} = \frac{(r_0)_{Cs} + (r_0)_{Ar}}{2} = \frac{(3.418)\,\text{Å} + (5.159)\,\text{Å}}{2}$$

$$r_{12} = 4.289\ \text{Å}$$

Use eqn. (5-29):

$$D_6 = \frac{B\,T^{3/2}\sqrt{\left(\frac{1}{M_1}\right) + \left(\frac{1}{M_2}\right)}}{P\,r_{12}^2\,\Omega_D}$$

$$= \frac{(1.040\times10^{-3})(643\,K)^{3/2}\left[\frac{1}{132.91} + \frac{1}{39.95}\right]^{1/2}}{(0.015\,atm)(4.289\,\text{Å})^2(0.5236)}$$

$$D_6 = 19.67\ cm^2/sec$$

Derivation of diffusion equation: (steady-state)

Assumptions: 1) flat front between Argon & cesium
2) zero thickness condensate (cesium layer at the wall)
3) flat wall (neglect grooves)

Control Volume: